NATIONAL ADVISORY COMMITTEE FOR AERONAUTICS

TECHNICAL NOTE 3344

THEORETICAL AND EXPERIMENTAL INVESTIGATION OF
AERODYNAMIC-HEATING AND ISOTHERMAL HEAT-
TRANSFER PARAMETERS ON A HEMISPHERICAL
NOSE WITH LAMINAR BOUNDARY LAYER
AT SUPERSONIC MACH NUMBERS

By Howard A. Stine and Kent Wanlass

Ames Aeronautical Laboratory
Moffett Field, Calif.

NACA

Washington
December 1954

T

NATIONAL ADVISORY COMMITTEE FOR AERONAUT1

TECHNICAL NOTE 3344

THEORETICAL AND EXPERIMENTAL INVESTIGATION OF
AERODYNAMIC-HEATING AND ISOTHERMAL HEAT-
TRANSFER PARAMETERS ON A HEMISPHERICAL
NOSE WITH LAMINAR BOUNDARY LAYER
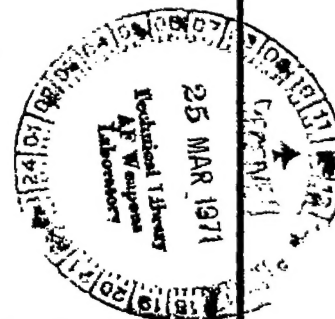AT SUPERSONIC MACH NUMBERS

By Howard A. Stine and Kent Wanlass

SUMMARY

The effect of a strong, negative pressure gradient upon the local
rate of heat transfer through a laminar boundary layer on the isothermal
surface of an electrically heated, cylindrical body of revolution with a
hemispherical nose was determined from wind-tunnel tests at a Mach number
of 1.97. The investigation indicated that the local heat-transfer para-
meter, $\mathrm{Nu}/\sqrt{\mathrm{Re}}$, based on flow conditions just outside the boundary layer,
decreased from a value of 0.65 ±0.10 at the stagnation point of the hemi-
sphere to a value of 0.43 ±0.05 at the junction with the cylindrical
afterbody. Because measurements of the static pressure distribution over
the hemisphere indicated that the local flow pattern tended to become
stationary as the free-stream Mach number was increased to 3.8, this dis-
tribution of heat-transfer parameter is believed representative of all
Mach numbers greater than 1.97 and of temperatures less than that of dis-
sociation. The local heat-transfer parameter was independent of Reynolds
number based on body diameter in the range from 0.6×10^6 to 2.3×10^6.

The measured distribution of heat-transfer parameter agreed within
±18 percent with an approximate theoretical distribution calculated with
foreknowledge only of the pressure distribution about the body. This
method, applicable to any body of revolution with an isothermal surface,
combines the Mangler transformation, Stewartson transformation, and thermal
solutions to the Falkner-Skan wedge-flow problem, and thus evaluates the
heat-transfer rate in axisymmetric compressible flow in terms of the known
heat-transfer rate in an approximately equivalent two-dimensional incompres-
sible flow.

Measurements of recovery-temperature distributions at Mach numbers
of 1.97 and 3.04 yielded local recovery factors having an average value
of 0.823 ±0.012 on the hemisphere which increased abruptly at the shoulder
to an average value of 0.840 ±0.012 on the cylindrical afterbody. This
result suggests that the usual representation of the laminar recovery
factor as the square root of the Prandtl number is conservative in the
presence of a strong, accelerating pressure gradient.

INTRODUCTION

Due to the processes of friction and compression, a body moving through the atmosphere accumulates as thermal energy a portion of its mechanical energy of motion. The physiological, structural, and aerodynamic ramifications of this well-known fact in the realm of high-speed flight constitute the aerodynamic heating problem. The present status of knowledge insofar as the aerodynamic aspects are concerned will be discussed in the following section. It is sufficient now to state on the basis of a review of selected literature (refs. 1 through 25) that the heat transfer through the surface of a supersonic vehicle can be predicted with confidence only when the heat path is through regions of laminar flow and small pressure gradient. Because in supersonic flow a constant-pressure surface has a sharp leading edge which is difficult, if not impossible to cool (refs. 15 and 16), the practical vehicle for sustained supersonic flight may, of necessity, be blunt. Although favorable to the promotion of laminar flow, the severe pressure gradients associated with bluff bodies can result in heat-transfer rates quite different from those on constant-pressure surfaces. The heat-transfer characteristics of the compressible boundary layer on bluff bodies are therefore required.

The present investigation has as its purpose the measurement in supersonic flow of laminar-boundary-layer temperature-recovery factors and local heat-transfer coefficients on the uniformly heated surface of a hemisphere-cylinder. The experimental results are compared with a newly developed method of approximate prediction which utilizes existing solutions to the boundary-layer problem, and which is applicable to any bluff body of revolution with an isothermal surface.

ANALYSIS

Status of Knowledge

The ultimate rate of heat transfer through a given type of boundary layer (i.e., laminar or turbulent) has been found to depend upon the fluid flow conditions characterized by Mach number and Reynolds number, the fluid properties specified by Prandtl number, the surface temperature distribution, and the body shape. In order to calculate the heat-transfer rate from boundary-layer theory, the body surface is commonly assumed to be a flat plate or axisymmetric. Effects of body curvature upon the pressure distribution normal to the surface are neglected, and body-shape effects are assumed to depend on the streamwise pressure distribution alone. When dealing with bodies of revolution, an additional shape parameter must be considered which accounts for the variation of circumference along the axis. However, because this additional shape parameter has been shown to relate the axisymmetric boundary-layer flow with an associated

two-dimensional flow (ref. 2), it is possible, without loss in generality, to apply two-dimensional results to axisymmetric bodies.

A representative sample of the extensive literature dealing with laminar-boundary-layer heat-transfer theory is given in references 3 through 11. The large body of analysis based upon integral methods of solution has been excluded from this survey partly in the interests of brevity, and partly because the accuracy of these integral analyses is judged by comparison with solutions such as those of references 3 through 11. Fluid-property and flow-parameter effects are stressed in references 3, 4, and 5. Nonisothermal surfaces are considered in reference 6. Pressure gradient effects are studied in references 7 and 8. Effects of small pressure and wall-temperature gradients are investigated in reference 9. Both pressure-gradient and fluid-property variations are considered in reference 10, and pressure-gradient and wall-temperature effects are discussed in reference 11. The results of these studies suggest that fluid-property and flow-parameter variations exert a relatively mild influence on the local heat-transfer coefficient. Pressure and wall-temperature gradients, on the other hand, can produce local heat-transfer coefficients which depart significantly from the isobaric and isothermal predictions. The influence of shape is illustrated in reference 12 - which, incidentally, presents an excellent account of methods employed to predict heat transfer - wherein a procedure is developed for the calculation of laminar heat-transfer coefficients about isothermal cylinders of arbitrary cross section. The effect of nonuniform temperature upon the heat-transfer coefficient in an application of practical interest is assessed in reference 13, which is a study of transient heating in a flat plate.

Accurate experimental verification of the laminar heat-transfer theory has been obtained in cases where the surface temperature and pressure were nominally uniform (refs. 14 through 17). Heat-transfer measurements under conditions of nonuniform temperature are discussed in reference 18. References 19 and 20 describe experiments in which local heat-transfer coefficients were measured in supersonic flow on nominally isothermal bodies with negative pressure gradients. In the former case the pressure gradient was mild and the heat-transfer coefficient did not depart significantly from the theoretical prediction for a constant-pressure surface. On the other hand, in the latter experiment, the heat-transfer coefficient was a strong function of the relatively severe pressure gradient; however, since the data of reference 20 were obtained under transient conditions in the presence of a surface temperature tending to become nonisothermal, the validity of these results is uncertain.

Heat Transfer

According to the Newtonian Law of heat transfer, the thermal flow through a unit area of the fluid in contact with an isothermal surface is proportional to the difference between the actual skin temperature and the skin temperature corresponding to no heat flow. The factor of

proportionality, called the local heat-transfer coefficient, depends,
in cases of forced convection, upon the boundary-layer type, and the
flow, fluid-property, and pressure-gradient parameters mentioned pre-
viously. For laminar flow, the local Nusselt number formed from the
local heat-transfer coefficient, the length of boundary-layer run, and
the local free-stream thermal conductivity can be combined with the local
Reynolds number into a local heat-transfer parameter, defined as the ratio
of the Nusselt number to the square root of the Reynolds number:

$$\frac{Nu}{\sqrt{Re}} \equiv \frac{hx/k_1}{\sqrt{\dfrac{\rho_1 u_1 x}{\mu_1}}} \tag{1}$$

(For Notation, see Appendix A.)

On the basis of available theory for isothermal surfaces, moderate
Mach number, and small temperature differences, one can reason that the
local laminar heat-transfer parameter on the blunt nose of a body of
revolution should lie within the interval $0.66 \geq Nu/\sqrt{Re} \geq 0.30$. The higher
value (at the stagnation point of a sphere) is predicted (for $\sigma = 0.7$)
in reference 22 by neglecting compressibility; the lower figure is appli-
cable to a flat plate or a hollow cylinder with surface parallel to the
air stream.

No exact, simple expression can be written to predict the local heat-
transfer parameter for points on the surface of a body lying in regions
of arbitrary pressure gradients, although a number of approximate methods
are available (refs. 12, 23, and 24 for example). Another approximate
method - an adaptation of a technique described in reference 12 - which
is easy to apply to any body of revolution and promises to be fairly
accurate for uniform surface temperatures not greatly different from the
stagnation temperature - was developed in conjunction with the present
experimental investigation. This method has the advantage that no knowl-
edge is required of the velocity or temperature profiles in the boundary
layer; only the pressure distribution about the body need be known. The
main results of this analysis are summarized in the following paragraphs;
the details can be found in Appendix B.

Briefly, the method makes use of the transformations of Mangler,
(ref. 2) and Stewartson (ref. 25) to remove the problem from the axisym-
metric compressible plane to the approximately equivalent two-dimensional
incompressible plane. The local heat-transfer parameter on the axisym-
metric body in compressible flow, $Nu/\sqrt{Re}$, is expressed in terms of the
corresponding parameters in two-dimensional incompressible flow, $\overline{\overline{Nu}}/\sqrt{\overline{\overline{Re}}}$,
and two-dimensional compressible flow, $\overline{Nu}/\sqrt{\overline{Re}}$, as follows:

$$\frac{Nu}{\sqrt{Re}} = \left(\frac{Nu/\sqrt{Re}}{\overline{Nu}/\sqrt{\overline{Re}}}\right)\left(\frac{\overline{Nu}/\sqrt{\overline{Re}}}{\overline{\overline{Nu}}/\sqrt{\overline{\overline{Re}}}}\right)\frac{\overline{\overline{Nu}}}{\sqrt{\overline{\overline{Re}}}} \qquad (2)$$

The factor relating axisymmetric and two-dimensional compressible flows (Mangler's transformation, ref. 2) is:

$$\frac{Nu/\sqrt{Re}}{\overline{Nu}/\sqrt{\overline{Re}}} = \sqrt{\frac{xr_o^2}{\int_{x_o}^{x} r_o^2\, dx}} \qquad (3)$$

This factor is specified completely by the shape of the body of revolution.

The factor arising from Stewartson's transformation (ref. 25) between two-dimensional compressible and incompressible flows is:

$$\frac{\overline{Nu}/\sqrt{\overline{Re}}}{\overline{\overline{Nu}}/\sqrt{\overline{\overline{Re}}}} = \sqrt{\frac{\overline{x}\left(\dfrac{\overline{a}_1}{\overline{a}_o}\right)^{\frac{s\gamma-1}{\gamma-1}}}{\displaystyle\int_{\overline{x}_o}^{\overline{x}}\left(\dfrac{\overline{a}_1}{\overline{a}_o}\right)^{\frac{s\gamma-1}{\gamma-1}} d\overline{x}}} \qquad (4)$$

This factor involves not only the streamwise body coordinate but also changes in the local speed of sound just outside the boundary layer and is rigorously valid only for vanishingly small heat transfer, Prandtl number of unity, and viscosity proportional to temperature. The consequences of relaxing the first two of these restrictions and the evaluation of this factor in terms of known conditions in the axisymmetric compressible flow are discussed in Appendix B.

To make practical use of equation (2) it is necessary to specify an incompressible heat-transfer parameter which corresponds to some known characteristic of the axisymmetric compressible flow. An approximate correspondence can be established if the boundary-layer model of Fage and Falkner is assumed for the incompressible plane. This wedge-flow model, in which both the local free-stream velocity and the surface temperature are proportional to arbitrary powers of the streamwise coordinate so that velocity and temperature profiles through the layer at all streamwise locations are similar, has been studied extensively. The local, incompressible heat-transfer parameter, $\overline{\overline{Nu}}/\sqrt{\overline{\overline{Re}}}$, has been calculated for the wedge flows over wide ranges of Prandtl number $\overline{\overline{Pr}}$, temperature-gradient parameter $\overline{\lambda}$, and pressure-gradient parameter $\overline{\overline{m}}$ (refs. 10 and and 11). According to this theory, the pressure-gradient parameter

and the temperature-gradient parameter are constant over the wedge and are related to the local flow, streamwise coordinate, and local surface temperature as follows:

$$\bar{\bar{m}} = \frac{d\bar{\bar{u}}_1}{d\bar{\bar{x}}} \frac{\bar{\bar{x}}}{\bar{\bar{u}}_1} \left. \right\}$$

$$\bar{\bar{\lambda}} = \frac{d\bar{\bar{T}}_s}{d\bar{\bar{x}}} \frac{\bar{\bar{x}}}{\bar{\bar{T}}_s} \left. \right\}$$

(5)

It has been shown (ref. 12, for example) that even though the pressure-gradient parameter $\bar{\bar{m}}$ varies as a function of the coordinate, $\bar{\bar{x}}$, the Fage and Falkner model can be applied locally to predict a corresponding variation of local heat-transfer parameter. The agreement with experiment is good, even though the theory is not rigorously applicable. The assumption is therefore introduced that the last factor on the right-hand side of equation (2) is defined on a local basis for a given Prandtl number and uniform surface temperature ($\bar{\lambda} = 0$) by local values of the incompressible pressure-gradient parameter, $\bar{m}$. For convenience and consistency it is further assumed that the incompressible pressure-gradient parameter has its analogues in the two-dimensional compressible and the axisymmetric compressible flows. The relation between pressure-gradient parameters in the respective flows is taken to be:

$$\bar{\bar{m}} = \left(\frac{\bar{\bar{m}}}{\bar{m}}\right) \left(\frac{\bar{m}}{m}\right) m$$

(6)

where

$$m \equiv \frac{du_1}{dx} \frac{x}{u_1} = \frac{dM_1}{dx} \frac{x}{M_1} \left(\frac{5}{5 + M_1^2}\right)$$

(7)

The right-hand side of equation (7) can be evaluated as a function of the coordinate x for a body of revolution about which the local isentropic flow is known. The transformation factors $(\bar{\bar{m}}/\bar{m})$ and $(\bar{m}/m)$ on the right-hand side of equation (6) can be calculated approximately in terms of the local flow about the body of revolution, as is shown in detail in Appendix B. Thus a correspondence is established between the known

pressure-gradient parameter, m, in the axisymmetric compressible plane and the analogous parameter, $\bar{\bar{m}}$, in the incompressible two-dimensional plane. One is therefore able to determine the last factor on the right-hand side of equation (2) by recourse to the tables of references 10 and 11; and, consequently, the distribution of axisymmetric compressible heat-transfer parameter $Nu/\sqrt{Re}$ can be established.

In the present investigation, the local heat-transfer-parameter distribution on the surface of a hemisphere-cylinder is calculated using the experimentally determined pressure-gradient parameter, m, according to the foregoing method.

Recovery Temperature and Recovery Factor

When a body moves through the atmosphere the surface tends to assume a temperature distribution, called the equilibrium temperature distribution, such that the local heat transfer at each point is a minimum. In the absence of radiation and internal heat flow the minimum heat transfer is zero; this equilibrium distribution is called the recovery-temperature distribution, and the body is said to be insulated. Since a spot on the surface can assume a temperature no greater than its local recovery temperature, the question of how hot a body can possibly become for given flight velocity and ambient temperature can be answered by investigating the properties of insulated bodies.

The recovery temperature at a point on an insulated body is specified by the sum of the local free-stream temperature just outside the boundary layer and the temperature rise across the boundary layer. The temperature rise across the boundary layer depends upon the boundary-layer type and the dimensionless flow, fluid property, and body-shape parameters mentioned previously. It is convenient to compare the actual temperature rise across the boundary layer with the rise which would occur if the local free stream were brought to rest adiabatically. In the notation of Appendix A, the ratio so obtained can be written

$$C_r = \frac{T_r - T_1}{T_t - T_1} \qquad (8)$$

The factor C_r is called the temperature-recovery factor and has a different value for laminar than for turbulent boundary layers.

With the aid of analogue computers and numerical integrations, the local laminar recovery factors on an insulated flat plate in air have been deduced (ref. 3, 4, and 5) for a wide range of local free-stream velocities and temperatures. It is interesting to note that one can correlate these

recovery factors as a function of the sum of the local free-stream temperature T_1 and the stagnation temperature, T_t, provided the air does not dissociate. The flow parameters (Mach number and Reynolds number) do not enter the correlation explicitly. If the sum of T_1 and T_t does not exceed about 2000° Rankine, the recovery factors predicted in references 4 and 5 can then be approximated within 1 percent by the following equation:

$$C_r = \sqrt{Pr\left(\frac{T_t + T_1}{2}\right)} \qquad (9)$$

where $Pr_{(T_t + T_1/2)}$ is the Prandtl number evaluated at the arithmetic mean of the local free-stream and the stagnation temperatures. If the sum of T_1 and T_t is greater than 2000° Rankine, equation (9) does not hold, and it is desirable to utilize the predictions of references 3, 4, and 5 directly.

Although the influence of pressure gradient on the local laminar recovery factor has been calculated theoretically for two-dimensional, constant-property wedge flows, slight disagreement exists among the numerical results of four independent determinations of the recovery factor at a stagnation point (ref. 21). The extremes of the various computations range from a prediction of no change to a prediction of a 5-percent decrease in recovery factor from the constant-pressure value. Thus, the validity of equation (9) in regions of nonzero pressure gradient can best be determined by experiment.

In the present investigation the equilibrium-temperature distribution on the surface of a hemisphere with a cylindrical afterbody was measured, assumed to be the recovery-temperature distribution, and combined with the local free-stream temperature and the stagnation temperature according to equation (8) to test the applicability of equation (9) in a strong pressure gradient. For reasons to be discussed later, the equilibrium temperature close to the stagnation point of the test body was significantly different from the recovery temperature. Hence, in this region the recovery factor was estimated by combining the theoretical results of references 4 and 5 with that of reference 21 which produced the best fit with the valid portion of the data. Once the recovery factor was known, the recovery temperature (necessary for reduction of heat-transfer data) was found from equation (8) rewritten:

$$\frac{T_r}{T_t} = \frac{T_1}{T_t} + C_r\left(1 - \frac{T_1}{T_t}\right) \qquad (10)$$

APPARATUS AND PROCEDURE

Wind Tunnels

The present experimental investigation was conducted in the Ames 1- by 3-foot supersonic wind tunnels No. 1 and No. 2. Wind tunnel No. 1 is of the closed-circuit, continuous-operation, variable-pressure type and is equipped with a flexible-plate nozzle that provides a range of Mach numbers from 1.2 to 2.5. The absolute pressure in the tunnel settling chamber can be varied from one-fifth of an atmosphere to three atmospheres to provide changes in the test Reynolds number. The absolute humidity of the air is maintained at less than 0.0001 pound of water per pound of dry air so that the effects of water vapor on the supersonic flow are negligible. The No. 2 wind tunnel is of the intermittent-operation, nonreturn, variable-pressure type and uses the dry air at high pressure (six atmospheres absolute) from the Ames 12-foot wind tunnel. The air is expanded to atmospheric pressure through the 1- by 3-foot test section, which is structurally identical to that of wind tunnel No. 1. The Mach number can be varied from about 1.2 to 3.8. The steady running time available for each test depends largely on the test Mach number and varies from about 18 minutes at a Mach number of 2.9 to 5 minutes at a Mach number of 3.8. The total pressure in the wind-tunnel settling chamber is controlled by means of a butterfly throttling valve in the supply pipe. Because the air in the supply system expands during each test, the stagnation temperature decreases with time; the maximum rate of decrease is about 4° F per minute. Although thermal equilibrium is never achieved, it is possible to obtain valid temperature data under certain operating conditions. Wind tunnel No. 2 was used for some of the tests because it provides higher Mach numbers and Reynolds numbers than wind tunnel No. 1.

Test Body

A hemispherical nose shape was selected for the test body in the present investigation. Considerations of experimental convenience (such as ease of construction, mounting, and testing) and the precedent of considerable theoretical background dealing with flow about spheres combined to suggest the hemisphere as the test body. The 4-inch diameter hemispherical nose had a cylindrical afterbody with a length limited to 3 inches to avoid intersecting the reflection of the bow shock wave from the wind-tunnel walls. Three sting-supported models of the test body were constructed, each having the same external size and shape, and surface roughnesses (less than about 20 microinches). The instrumentation housed in each and the sting-support details, however, were different.

Pressure-distribution model.- The pressure-distribution model (fig. 1(a)) made from aluminum, had a wall thickness of one-half inch. Twenty-two 0.031-inch-diameter static-pressure orifices were placed on the surface in a plane passing through the axis of revolution (meridian plane). Brass plugs containing the drilled orifices were pressed

into 3/16-inch-diameter, 3/8-inch-deep holes in the aluminum. Copper
tubing attached to the plugs passed radially through 0.064-inch-diameter
holes into the model cavity and emerged through a 2-inch-diameter hollow
sting threaded into the base. Each plug and tube was coated with an
alkyd resin before insertion to prevent leaks between the cavity and the
surface.

Recovery-temperature model.- The recovery-temperature model
(fig. 1(b)), made from stainless steel, had, except for the afterbody,
a nominal wall thickness of 0.020 inch. The thickness of the cylindrical
portion increased linearly from 0.020 inch at its junction with the hemi-
sphere (shoulder) to 1/8 inch at the point of attachment of the 1/2-inch-
thick base ring. The thin wall served to minimize both the heat capacity
of the model and the longitudinal heat conduction within the shell.
Stainless steel was used because of its low thermal conductivity relative
to other metals. Twenty-four constantan wires were soldered into holes
in the surface lying in a meridian plane, as shown in figure 1(b). A
single stainless-steel wire connected to the inside of the shell near
the base completed the return circuit for the twenty-four stainless-
steel-constantan thermocouples. The thermocouple wires were brought into
the 2-inch-diameter hollow sting through a pressure-tight fitting in the
base. The assembly was calibrated in a liquid bath. A copper tube com-
municating with the model cavity was provided so that the internal air
pressure could be reduced to less than 400 microns (0.016-inch Hg) abso-
lute to minimize internal heat transfer due to free convection.

Heat-transfer model.- The heat-transfer model (fig. 1(c)) was a
stainless-steel shell which formed the resistance element of the low-
voltage, high-amperage electrical circuit used to heat the body. The
circuit was arranged so that a 60-cycle alternating current could be passed
longitudinally through the shell, entering through a copper bus bar imbed-
ded in the nose, and leaving through a copper collector ring which formed
the base. The interior surface of the shell was contoured to provide an
effective thickness distribution, and therefore a resistance distribution,
which was proportional to the expected heat-removal capabilities of the
air stream when the temperature was uniform. Twenty-two copper-constantan
thermocouples were soft-soldered in holes drilled through the shell in a
meridian plane, with the thermocouple junctions within 1/32 inch of the
outer surface. The spacing is indicated in figure 1(c). The wires ter-
minated at a selector switch outside the wind tunnel which was arranged
so that, on alternate sides of the body, succeeding pairs of the copper
wires which formed one side of each copper-constantan thermocouple cir-
cuit could be utilized as taps to measure the A.C. voltage drop existing
along any 12° arc on the hemisphere. A simultaneous indication of tem-
perature could be obtained from the thermocouple lying within the same
interval but displaced 180° about the axis. The stations on the afterbody
were spaced the same distance apart as were those on the hemisphere. To
prevent heat generated in the nose from flowing by conduction into the
3/4-inch-diameter copper feeder bus bar, an independently controlled elec-
trical heating coil, wound on an aluminum spool, surrounded the bus bar.

The temperature within the bus bar was monitored with iron-constantan thermocouples, and the power supplied to the heater was adjusted to minimize the temperature gradient in the bus bar between the shell and the heater.

A photograph of the heat-transfer model installed in wind tunnel No. 1 is shown in figure 1(d).

Instrumentation and Accuracy

The experimental data leading to evaluation of the recovery factors consisted of pressure and temperature measurements. Static and total pressures were measured by conventional methods with a relative error of ±1 percent in the worst case. Temperatures were obtained from thermocouple voltages sensed on either indicating or recording potentiometers that were accurate to ±0.25° F. However, in wind tunnel No. 1 an additional uncertainty, due to a ragged temperature distribution in the settling chamber, limits the probable accuracy of the temperature determinations in this wind tunnel to ±1.5° F. In the worst case the relative error of the temperature determination was ±0.5 percent. Heat transfer due to radiation was estimated and found to be negligible.

The evaluation of Nusselt number required, in addition to pressures and temperatures, the measurement of the local voltage drops along the model surface and the total current flowing in the electrical heating circuit. Local voltage drops, which ranged from 0.0025 to 0.03 volts, A.C., were measured with an electronic voltmeter having a relative error of ±3 percent. The current, which varied from 650 to 900 amperes, was measured with a relative error of ±1 percent.

The actual centers of the measuring stations on the test bodies corresponded to the nominal locations (fig. 1) within ±0.005 inch. Surface areas of the segments on the heat-transfer body were calculated using the nominal nose radius of 2 inches and the nominal station locations. The fluid properties of viscosity and thermal conductivity corresponding to the calculated local static temperatures were taken from curves prepared from the tables of reference 26.

The probable error of the principal parameters, based on the probable error with which each individual component could be determined, can be summarized as follows:

	Percent
Mach number, M	±1
Reynolds number, Re	±1
Recovery factor, C_r	±1.5
Nusselt number, Nu	±15

The precision of the recovery-factor measurement, which is somewhat less than that possible on a constant-pressure surface, includes an uncertainty due to heat conduction in the shell of the test body. Likewise, the accuracy of the Nusselt number measurement includes an allowance for slight nonuniformity of the heated-surface temperature.

Tests

Each test body was oriented in the wind tunnels so that the meridian plane containing the instrumentation coincided with the vertical plane of the test sections. All bodies were adjusted to an angle of attack of 0° $\pm0.1^\circ$. Axial location in the tunnels was selected on the basis of wind-tunnel-calibration data to minimize effects of local-pressure-gradient and stream-angle variations. Observations with schlieren optical systems indicated that the boundary layers on the hemispheres were laminar for all test conditions in both wind tunnels. Wind-tunnel conditions for each series of tests are given in table I.

Pressure-distribution tests.- Static-pressure distributions obtained in wind tunnels No. 1 and No. 2 were converted to local Mach number variations about the body. Isentropic flow was assumed to exist behind the bow shock wave in the stream tube just outside the boundary layer; the static pressure across the boundary layer was assumed to be constant so that $p_s = p_1$. To check the isentropic-flow assumption, an impact tube formed from stainless-steel tubing was soldered into the rearmost orifice on the afterbody. This tube was situated so that the mouth was normal to, and one-eighth inch from the body surface, and at the same station as the preceding static orifice. Schlieren-system observations verified that the opening was just outside the boundary layer at all Reynolds numbers. The impact and static-pressure measurements at this station allowed, with the aid of Rayleigh's pitot-tube equation, independent determinations of local Mach number which agreed well with those obtained with the isentropic flow assumption.

A check run in wind tunnel No. 1 with the pressure orifices in the horizontal plane (1-foot dimension in wind tunnel) revealed no flow asymmetries.

Temperature-distribution tests.- In wind tunnel No. 2, the surface-to-stagnation-temperature ratios at all stations ceased to change as a function of elapsed testing time after an interval of about seven minutes. This was taken as an indication that the starting transient had died away and that a quasi-steady state of thermal equilibrium existed on the test-body surface. No data which were considered valid could be obtained at a test Mach number of 3.8 because the duration of run did not exceed 5 minutes. The possible errors due to the small but finite heat transfer which accompanied the stagnation-temperature drift were evaluated at $M_\infty = 1.97$ by comparing the constant values of the surface-to-stagnation-temperature ratios obtained in the intermittent-operation wind tunnel (No. 2) with those obtained under steady-state conditions in the

continuous-operation wind tunnel (No. 1) at nearly the same test Reynolds number. This comparison disclosed that the agreement was good except close to the nose of the test body.

In wind tunnel No. 1 the steady-state value of the surface-to-stagnation-temperature ratio at the stagnation point of the hemisphere did not reach unity. To determine if this were caused only by heat losses in the shell (conduction and internal free convection), or could possibly be due also to nonadiabatic compression along the stagnation streamline, the constantan wire at the stagnation point was replaced with a sleeve of 1/16-inch-O.D. stainless steel tubing having a length of approximately 1/2 inch. The sleeve was flush with the outer surface and provided support for a 30-gage, glass-insulated, iron-constantan duplex thermocouple wire which was slipped through from the interior of the model. The 1/32-inch-diameter junction, which was approximately spherical, was cantilevered upstream on a 1/4-inch-long bared portion of the 0.010-inch-diameter thermocouple wires. The axial location of the junction could be varied by sliding the insulating sheath in the sleeve. The temperature obtained from this thermocouple was closer to the wind-tunnel stagnation temperature than it was to the temperature measured by the thermocouples imbedded near the nose of the model shell, showing that due to heat conduction, the true recovery temperatures were not obtained near the stagnation point.

Heat-transfer tests.- The heat-transfer experiments were carried out under steady-state conditions in wind tunnel No. 1. The heating current which produced the most uniform surface temperature was found experimentally at each test Reynolds number, at which time the local voltage drop and surface-temperature distributions were recorded. The local Nusselt number was formed from the measured quantities as follows:

$$Nu \equiv \frac{hx}{k_1} = \frac{qx}{(T_s - T_r)k_1} = \frac{dQ}{dA}\left(\frac{x}{k_1}\right)\frac{1}{T_s - T_r} \approx \frac{\Delta Q}{\Delta A}\left(\frac{x}{k_1}\right)\left(\frac{1}{T_s - T_r}\right)$$

$$\approx \frac{\kappa I \Delta E}{\Delta A(T_s - T_r)}\left(\frac{x}{k_1}\right) \qquad (11)$$

Because it was the purpose of this investigation to isolate the effect of pressure gradient upon the local heat-transfer parameter from the nonuniform temperature effect, considerable effort was expended in obtaining a constant surface temperature. Four trials were required to achieve a heating distribution which yielded a reasonably isothermal surface. The thickness distribution (resistance distribution) of the shell and the method of joining the feeder bus bar to the nose were improved between trials on the basis of the experimental results of each previous test. The shape of the inner surface in the vicinity of the stagnation point (fig. 1(c)) was a contour with the equation of a streamline obtained

from the solution of a well-known problem in potential flow - the flow inside the sphere obtained when a space doublet is combined with a uniform stream. The soft-soldered joint between the copper bus bar and the stainless-steel shell was made on the equipotential surface passing through the stagnation point.

Because the inner surface of the shell could not be machined to the desired contour with the required accuracy, the resistance was corrected to within ±10 percent of the desired distribution by a process of selective electroplating with copper. The technique employed was as follows: After chemical cleaning, the inaccurately contoured model was supported nose down, and the interior, unobstructed except for the feeder bus bar, was electroplated with a flash-coat of nickel, followed immediately by a flash of copper deposited from a cyanide electrolyte. Provision was then made for filling the interior to any desired level with carbon tetrachloride supporting a film of copper sulphate solution approximately 1/8 inch deep. With a washer-like anode of copper suspended in the electrolyte, an annular band of copper could be deposited or removed from any desired elevation on the inner surface of the model. When a small current was passed through the heating circuit, plating progress could be observed and controlled by measuring the change in voltage drop between externally mounted taps.

RESULTS AND DISCUSSION

The results of the local static-pressure, recovery-temperature, and heat-transfer measurements on the 4-inch hemisphere-cylinder are presented in figures 2 through 4 with the distance along the surface in a meridian plane (arc length) as the independent variable. The arc length x is normalized with respect to the body diameter D. The test Mach number M_∞ is that of the free stream; the test Reynolds numbers Re_D are based on conditions in the free stream, with the body diameter as the reference length. Local parameters, (M_1, Re, Nu, etc.) are based on conditions in the local flow just outside the boundary layer. The reference length, where required, is the arc length x.

Pressure Distribution

The static-pressure distributions measured about the hemisphere-cylinder at test Mach numbers of 1.97, 3.04, and 3.80 in wind tunnel No. 2 are presented in coefficient form in figure 2(a). The pressure coefficients about a sphere for inviscid incompressible flow, and for compressible flow at a Mach number of infinity according to Newtonian theory (ref. 27) are included for comparison. The measured pressure coefficients were independent of Reynolds number throughout the range covered. The size of symbols at each station (fig. 2(a)) outlines the extent of the experimental scatter and variation with Reynolds number. Although not evident from the figure, orifices lying between locations from $x/D = 0.35$

to $x/D = 0.45$ encompassed the sonic zone on the hemisphere and tended
to give erratic pressure indications unless each hole was carefully
cleaned of minute deposits of foreign matter. The values of pressure
coefficients obtained from the tests in wind tunnel No. 1 fall within
the symbols drawn around points obtained at the same Mach number in wind
tunnel No. 2. The pressure distribution obtained in wind tunnel No. 1
with the orifices in a horizontal plane agreed with that obtained with
the orifices in a vertical plane.

The local Mach number distributions derived from the pressure-
coefficient data and the Newtonian theory (ref. 27) are presented in
figure 2(b). Also included are the results of the determination of local
Mach numbers (at $x/D = 1.16$) by impact and static-pressure measurements.
The two methods of measurement agree within 1.5 percent in the worst case.

A tendency is noted in figure 2(b) for the increase in local Mach
number at a given station x/D to become progressively less as the Mach
number of the oncoming stream M_∞ is increased by an approximately fixed
increment. This trend is in accordance with the theory of reference 28,
which predicts that the entire flow pattern about an arbitrary body tends
to become stationary as the free-stream Mach number is increased. More-
over, because the significant (hypersonic similarity) parameter is a
function of the product of the thickness ratio and the Mach number, the
flow pattern about a bluff body "freezes" at a lower value of the Mach
number than is the case for a slender body. Because in the case of the
hemisphere-cylinder the local Mach number curves are similar in shape,
the pressure-gradient parameter m (eq. (7)) is a function principally
of the arc length, x/D, and depends but little upon the Mach number of
the oncoming stream. Hence, any dependence of the local heat-transfer
coefficient upon the free-stream Mach number and upon the pressure-
gradient parameter would be expected to become smaller and smaller as M_∞
increases.

Temperature Distributions and Recovery Factor

Typical temperature distributions obtained from the recovery-
temperature model in wind tunnel No. 1 at a test Mach number of 1.97 are
presented in figure 3(a). The temperature measured with an isolated
thermocouple projecting 1/16-inch upstream of the stagnation point
(plotted at $x/D = 0$; $T_O/T_t = 1.0000 \pm 0.0013$) indicates that the reduced
temperature near the nose of the unheated surface is due to conduction
in the model shell. The two experimental distributions shown correspond
to the two highest test Reynolds numbers and, accordingly, the least
serious conduction effects. They illustrate the extent to which conduction
influenced the equilibrium temperatures near the stagnation point under
the two most favorable test conditions. The coalescence of these two
curves at values of x/D greater than 0.35 was taken as an indication
that the equilibrium-temperature distribution beyond this point was a
close approximation to the recovery-temperature distribution. Also pre-
sented in figure 3(a) are temperature distributions obtained from the

heat-transfer model with power inputs adjusted to produce the most uniform surface temperatures.

The temperature-recovery factors (fig. 3(b)) computed from the equilibrium-temperature data (fig. 3(a)) and the local Mach number data (fig. 2(b)) are inaccurate for values of x/D less than about 0.35 for the reasons outlined above. The recovery factors measured at a Mach number of 1.97 in the intermittent-operation wind tunnel (No. 2) agree well with those obtained from measurements in the continuous-operation wind tunnel (No. 1) for values of x/D between 0.35 and 0.90. The recovery factors on the hemisphere have, for x/D greater than 0.35, a mean value of 0.823 ±0.012 which rises on the afterbody to a mean of 0.840 ±0.012 in the case of wind tunnel No. 1. The increasing recovery factors measured on the cylindrical afterbody at values of x/D greater than about 1.1 in wind tunnel No. 2 are believed to signify the onset of transition to turbulent flow. The recovery factor at $M_\infty = 3.04$ is lower than that at $M_\infty = 1.97$. This decrease may be due to the slightly more severe pressure gradient at $M_\infty = 3.04$; however, the difference is of the same order of magnitude as the probable accuracy of the measurements.

Also included in figure 3(b) are the recovery-factor predictions for a Mach number of 1.97 of constant-pressure variable-property theory, and of an empirical combination of constant-pressure theory and pressure-gradient theory for laminar flow derived below. The curve representing the constant-pressure theory was obtained from a graph prepared from the recovery-factor information given in references 4 and 5. Values of the recovery factor were selected from the graph to correspond with the known stagnation and local static temperatures of the test. This method, corresponding to the dashed curve (fig. 3(b)), predicts a slight increase of recovery factor with arc length on the hemisphere-cylinder, and it agrees well with the data for the cylindrical afterbody, but lies slightly above the data for the hemisphere. Although the recovery factor defined by a mean line passed through the valid portion of the data on the hemispherical nose is not more than 2 percent below the recovery factor for the cylindrical afterbody, and, consequently, the effect of pressure gradient can probably be disregarded in practice, the decrease in level can be predicted very closely, at least in the case of the hemisphere at $M_\infty = 1.97$, by an empirical method which was used to compute the solid curve presented in figure 3(b). This latter recovery-factor curve, which was subsequently utilized to calculate recovery temperatures (eq. (10)) for the reduction of heat-transfer data, was obtained as follows: Recovery factors computed for a constant-pressure surface were assumed to differ from those for the same flow conditions but with arbitrary pressure gradient by a factor depending only upon the pressure-gradient parameter m (eq. (7)). Further, the recovery factors tabulated in reference 21, which apply to two-dimensional incompressible flow, were assumed to vary linearly with the incompressible pressure-gradient parameter $\bar{m}$ between the tabulated values for $\bar{m} = 0$ and $\bar{m} = 1$. The empirical equation embodying these assumptions is written:

$$C_r = C_{r_{m=o}}(1 - b\bar{\bar{m}})$$

where

$$b = 1 - \frac{\bar{\bar{C}}_{r(\bar{\bar{m}}=1)}}{\bar{\bar{C}}_{r(\bar{\bar{m}}=o)}} \qquad (12)$$

The recovery factors predicted for the hemisphere-cylinder at $M_\infty = 1.97$ by equation (12) are shown as the solid curve on figure 3(b). A value of $b = 0.023$, corresponding to the calculations of Levy and Seban (ref. 21) was used. The appropriate values of $\bar{\bar{m}}$ were obtained from the local Mach number distribution (fig. 2(b)) and equation (6).

The recovery factors measured at a Mach number of 1.97 lie slightly above the predicted curve in the interval from $x/D = 0.525$ to $x/D = 0.70$. This local maximum can be traced to a bulge faintly discernible in the corresponding equilibrium-temperature distributions (fig. 3(a)) which covers the same interval of arc length. Although the reason for this bulge is not known, it was characteristic of all the equilibrium-temperature data, and, as will be seen later, corresponds to the zone on the heated hemisphere where the heat-transfer rate is a maximum. It can be concluded from figure 3(b) that the local recovery factor on the hemisphere-cylinder may be predicted within ±1 percent by the foregoing method.

Heat Transfer

The measure of success realized in obtaining an isothermal surface on the heat-transfer model has already been indicated in figure 3(a). The maximum variation of the measured surface temperatures about a mean line representing a constant temperature is about ±2.5° F at $M_\infty = 1.97$ and $Re_D = 2.3 \times 10^6$. The maximum gradient of surface temperature, which extends over about one-tenth of the instrumented length is about 80° F per foot. The temperature potential, $T_s - T_r$, varies continuously on the hemisphere from a minimum of 35° F at the stagnation point to a maximum of about 72° F at the shoulder. The heat-transfer data taken under the conditions of nonuniform surface temperature, which existed during the first three attempts to achieve an isothermal surface, yielded heat-transfer parameters which departed considerably from those obtained with the final shell configuration. The reasons for this are two-fold: First, the nonuniformity of surface temperature was accompanied by heat conduction within the shell which rendered invalid the assumption that heat generated locally was transferred into the stream locally (eq. (11)). This can be considered to be an experimental error. Second, as has been discussed in reference 6, the heat-transfer parameters for nonisothermal

surfaces are significantly different from those on constant-temperature surfaces because local conditions depend upon boundary-layer history; hence, the measurements contain large contributions due to the temperature nonuniformities. Although the results of the final attempt to obtain a uniform surface temperature are not entirely free from the foregoing effects, the surface temperature is believed to have been sufficiently uniform that valid conclusions can be drawn from the heat-transfer data.

The distribution of the local heat input along the surface of the shell which was built into the body is presented in figure 4(a). The incremental voltage drop across equal intervals of arc (normalized with respect to the voltage drop at the shoulder) is plotted as a function of x/D. The points represent the distribution measured in wind tunnel No. 1 at $M_\infty = 1.97$ throughout the Reynolds number range; the scatter is due to voltage-reading errors. The curve represents the theoretical variation which it was desired that the model should possess. It is emphasized that the experimental heat-input distribution was invariant (i.e., it could be reproduced under no-wind conditions and could not be altered during a run) and accurately defined the heat-transfer rate at a given location only when power input and exterior cooling conditions yielded an isothermal surface.

The measured local heat-transfer-parameter distribution, $Nu/\sqrt{Re}$, corresponding to the most uniform surface temperature conditions on the body, is compared in figure 4(b) with the distribution predicted by the present theory. The data depart from the predicted curve by values of ±18 percent at most. However, due to the approximations employed in its development, the theory is subject to errors of unknown magnitudes. The experimental results, on the other hand, have a known uncertainty of about ±15 percent. Upon comparison of the theoretical with the experimental distribution, it appears probable that the theoretical distribution provides a closer representation of the local isothermal heat-transfer parameter on the hemisphere-cylinder than does the experimental distribution because the data deviate from the predicted distribution both in magnitude and sense in a manner which is easily explained upon examination of figures 3(a) and 4(a). The data tend to lie above the predicted curve in zones where the built-in heat production was too great (fig. 4(a)) and the measured temperature potential was too low due to internal conduction (fig. 3(a)); and they tend to lie below the theoretical curve where the converse was true. For these reasons, and as a result of careful analysis of figure 4(b), it is believed that the theoretical curve contains an uncertainty of not more than ±7 percent.

The increasing scatter of the data at values of x/D less than 0.25 is caused by the decrease in local Nusselt number and local Reynolds number as the stagnation point is approached, while the absolute error of measurement remains fixed. Within the accuracy of measurement, however, the heat-transfer-parameter distribution on the hemisphere-cylinder is independent of test Reynolds number throughout the range covered.

Also shown in figure 4(b) are the theoretical isothermal-surface, local heat-transfer parameters for the stagnation point of a sphere (ref. 22), a cone-cylinder in supersonic flow (refs. 2 and 6), and a flat plate (ref. 6). The stagnation-point prediction of reference 22 agrees well with the data and is in excellent agreement with the forecast obtained by the present method. The comparison between the cone-cylinder theory and the hemisphere-cylinder theory illustrates the effect of favorable pressure gradient upon the local heat-transfer parameter, and indicates that the local heat-transfer parameter on the hemisphere decreases from a value at the stagnation point about 27 percent greater than that on the cone to a value at the shoulder about 20 percent less than on the cone. The conical tip selected for this comparison has a half-angle, α, of 39.5°, so that the shoulders of both bodies occur at $x/D = \pi/4$. The theoretical heat-transfer parameters on the cylindrical afterbody approach the flat-plate value asymptotically.

The tendency for the local flow pattern about the hemisphere-cylinder to become stationary as the free-stream Mach number is increased has already been noted. On the basis of this observation it was inferred that the distribution of isothermal local heat-transfer parameter about the hemisphere-cylinder also tends to become stationary as the free-stream Mach number is increased. The experimental results at a Mach number of 1.97 are for this reason expected to be representative of all higher free-stream Mach numbers, provided that temperatures do not exceed that of dissociation. Furthermore, because the local Mach numbers are not arbitrarily large, it appears that any theory capable of predicting boundary-layer characteristics for an arbitrary but constant Prandtl number can be applied with good results to the flow about a bluff body throughout a wide range of free-stream Mach numbers.

CONCLUSIONS

To determine the effects of strong pressure gradient upon aerodynamic heating and heat transfer, distributions of static pressure, recovery temperature, and isothermal-surface heat-transfer rate have been measured on a hemisphere-cylinder with laminar boundary layer in supersonic flow. Analysis of these data and comparison of the results with predictions of various theories prompt the following conclusions:

1. In accordance with the hypersonic similarity theory of Oswatitsch, the local flow pattern about the hemisphere tended to become stationary as the free-stream Mach number was increased to 3.8. Since the corresponding maximum local Mach number was only about 2.5, it appears that boundary-layer characteristics for bluff bodies in hypersonic flow can be adequately predicted by theories in which the Prandtl number is an arbitrary constant.

2. Although the recovery temperature did not exist close to the
stagnation point of the test body, due to longitudinal heat conduction
within the model shell, the results show that the strong favorable
pressure gradient tends to decrease the laminar recovery factor, based
on local flow conditions just outside the boundary layer, from the
constant-pressure value of 0.840 ± 0.012 on the afterbody to a value of
about 0.823 ± 0.012 on the hemisphere. This decrease could be predicted
within ± 1 percent by an empirical expression which combines the constant-
pressure variable-property calculations of Young and Janssen and of
Klunker and McLean with the constant-property wedge-flow calculations
of Levy and Seban. This result suggests that the usual approximation
of the laminar recovery factor by the square root of the Prandtl number
is conservative in flows having strong pressure gradients.

3. The isothermal heat-transfer parameter, $Nu/\sqrt{Re}$, based on local
flow conditions just outside the laminar boundary layer, was independent
of Reynolds number and agreed within about ± 18 percent with a method
of approximate prediction developed herein. This method, which requires
foreknowledge only of the pressure distribution about a body of revolu-
tion, predicts a distribution of local isothermal heat-transfer parameter
on the hemisphere-cylinder believed to be in error by not more than
± 7 percent. Because of the tendency for the local flow pattern to become
independent of the free-stream Mach number, it is believed that these
results are representative of all free-stream Mach numbers greater than
about 2 and at temperatures less than that of dissociation.

Ames Aeronautical Laboratory
    National Advisory Committee for Aeronautics
        Moffett Field, Calif., Sept. 1, 1954

APPENDIX A

NOTATION

A   area, sq ft

a   speed of sound, ft/sec

B   constant, $ft^{-\lambda}$

b   constant

C   constant

C_r recovery factor, $\dfrac{T_r - T_1}{T_t - T_1}$, dimensionless

C_p constant-pressure specific heat, ft^2/sec^2, ^{o}F

C_v constant-volume specific heat, ft^2/sec^2, ^{o}F

D   diameter, ft

E   electrical potential, volts A.C. rms

f   boundary-layer stream function, dimensionless

G   constant

g   acceleration of gravity, ft/sec^2

h   heat-transfer coefficient, $\dfrac{q}{T_s - T_r}$, ft-lb/sec, ft^2, ^{o}F

I   electrical current, amp. A.C. rms

K   thermal conductivity coefficient (body), ft-lb/sec, ft, ^{o}F

k   thermal conductivity coefficient (air), ft-lb/sec, ^{o}F, ft

M   Mach number, $\dfrac{u}{a}$, dimensionless

m   pressure-gradient parameter, $\dfrac{du_1}{dx} \dfrac{x}{u_1}$, dimensionless

Nu   Nusselt number, $\dfrac{hx}{k_1}$, dimensionless

p   pressure, lb/ft^2

Pr   Prandtl number, $\dfrac{c_p \mu}{k}$, dimensionless

Q   average heat-transfer rate, $\int q\,dA$, ft-lb/sec

q   heat-transfer rate per unit area, $\left(-k\,\dfrac{\partial T}{\partial y}\right)_s$, ft-lb/sec, sq ft

Re   local Reynolds number, $\dfrac{\rho_1 u_1 x}{\mu_1}$, dimensionless

Re_D test Reynolds number, $\dfrac{\rho_\infty u_\infty D}{\mu_\infty}$, dimensionless

R   gas constant, ft^2/sec^2, $^\circ F$

r_O distance from axis of revolution to body surface, ft

r   radius, ft

S   boundary-layer temperature function, dimensionless

s   boundary-layer temperature ratio, $\dfrac{S}{S_s}$, dimensionless

T   absolute temperature, $^\circ F$

t   shell thickness, ft

u   velocity, ft/sec

V   velocity in transformed coordinate system, ft/sec

v   velocity normal to surface, ft/sec

x   distance from nose along body generator, ft

Y   transformed variable normal to surface, $sec^{1/2}$

y   space coordinate normal to body surface, ft

z   transformed coordinate parallel to surface, ft

α cone half-angle, deg

β constant, $\dfrac{ft^{1-m}}{sec}$

γ specific heat ratio $\left(\dfrac{c_p}{c_v} = 1.4\right)$, dimensionless

Δ indicates finite-difference approximation to differential operator

η boundary-layer coordinate normal to surface, dimensionless

κ constant, ft-lb/watt, sec

λ exponent in surface-temperature-distance relation, dimensionless

μ absolute viscosity, lb-sec/ft^2

ν kinematic viscosity, $\frac{\mu}{\rho}$, ft^2/sec

ρ mass density, slugs/ft^3

ψ stream function, ft/sec$^{1/2}$

Subscripts

t   stagnation condition

∞ main-stream condition

o   reference condition

1   local condition just outside boundary layer

s   local condition on body surface

e   equilibrium, surface-temperature condition

r   recovery, surface-temperature condition

Quatities provided with two bars refer to two-dimensional incompressible flow; quantities provided with one bar refer to two-dimensional compressible flow; unbarred quantities refer to axisymmetric compressible flow.

APPENDIX B

APPROXIMATE CALCULATION OF LAMINAR HEAT-TRANSFER PARAMETERS

ABOUT BODIES OF REVOLUTION IN SUPERSONIC FLOW

The purpose of this appendix is to describe an approximate means for calculating the local heat-transfer-parameter distribution about any iso-thermal body of revolution with laminar boundary layer. This method was used to obtain the theoretical curve given in figure 4(b) and to design the hemisphere-cylinder model employed in the present heat-transfer experiments. The method can best be described as a synthesis of existing laminar-boundary-layer theories and empirical observation which leads to a rapid estimate of the heat-transfer-parameter distribution for any iso-thermal body of revolution about which the local flow pattern is known.

The problem consists of evaluating equation (2) of the text by employ-ing the transformations of Mangler and Stewartson, so that the heat-transfer parameter in axisymmetrical compressible flow can be handled in terms of known incompressible-flow solutions in plane two-dimensional flow. Certain inconsistencies arise in the analysis because (a) Stewartson's transformation between the two-dimensional compressible and the two-dimensional incompressible flows does not hold exactly for Prandtl numbers other than unity and nonzero heat transfer, and (b) the pressure-gradient parameters of the wedge-flow solutions which are employed to specify the incompressible heat-transfer parameters become, in general, functions of the streamwise coordinates as a result of the transformations. The nature of the former inconsistency is examined below, and limits are tentatively proposed within which Stewartson's transformation may be expected to be useful. Justification for ignoring the latter inconsistency can be found in the fact that the incompressible heat-transfer-parameter distribution on bodies other than wedges can be predicted closely by local applications of wedge-flow solutions, and there is no a priori reason to expect the contrary for compressible flows.

The laminar-boundary-layer equations for compressible flow about a body of revolution alined with the stream are:

continuity:

$$\frac{\partial}{\partial x}(\rho r_0 u) + \frac{\partial}{\partial y}(\rho r_0 v) = 0 \qquad \text{(B1a)}$$

momentum:

$$\rho\left(u\,\frac{\partial u}{\partial x} + v\frac{\partial u}{\partial y}\right) = -\frac{dp}{dx} + \frac{\partial}{\partial y}\left(\mu\frac{\partial u}{\partial y}\right) \qquad \text{(B1b)}$$

energy:

$$\rho c_p \left(u \frac{\partial T}{\partial x} + v \frac{\partial T}{\partial y} \right) - u \frac{dp}{dx} = \frac{\partial}{\partial y}\left(k \frac{\partial T}{\partial y} \right) + \mu \left(\frac{\partial u}{\partial y} \right)^2 \qquad \text{(B1c)}$$

state:

$$p = \rho RT \qquad \text{(B1d)}$$

The equations for two-dimensional compressible flow are equivalent to equations (B1) with $r_0 = r = $ constant; and the equations for two-dimensional incompressible flow embrace, in addition, the stipulations that the density, ρ, viscosity, μ, and thermal conductivity, k, are invariant, and that the temperature is independent of the pressure.

Relation Between Axisymmetric Compressible Flow and Two-Dimensional Compressible Flow

Mangler (ref. 2) has shown that equations (B1) can, by means of the coordinate transformation

$$\overline{x} \quad \propto \quad \int_{x_0}^{x} r_0^2(x)\,dx \qquad \text{(B2a)}$$

$$\overline{y} \quad \propto \quad r_0(x) \cdot y \qquad \text{(B2b)}$$

be cast into the equations for two-dimensional compressible flow. By utilizing equation (1) of the text and appropriate definitions given in Appendix A in conjunction with Mangler's transformation it is not difficult to discover that

$$\frac{Nu}{\sqrt{Re}} = \frac{\overline{Nu}}{\sqrt{\overline{Re}}} \sqrt{ \frac{r_0^2 \cdot x}{\int_{x_0}^{x} r_0^2\,dx} } \qquad \text{(B3)}$$

Equation (B3) provides a representation of the axisymmetric compressible heat-transfer parameter in terms of a corresponding plane two-dimensional compressible parameter which is exact within the scope of boundary-layer theory.

Two limiting cases can be calculated for any body of revolution having a cylindrical afterbody and a bluff forebody such that r_0 increases monotonically with x. Sufficiently near the stagnation point the forebody approximates a disc normal to the stream so that $r_0 = x$. An evaluation of the radical on the right-hand side of equation (B3) for this condition gives the result that the heat-transfer parameter at the stagnation point is $\sqrt{3}$ times the heat-transfer parameter for a certain corresponding body in a two-dimensional compressible flow. On the cylindrical afterbody, $r_0 = r = $ constant, and equation (B3) yields the result:

$$\frac{\overline{Nu}/\sqrt{\overline{Re}}}{Nu/\sqrt{Re}} = \sqrt{\frac{\int_0^{x=F(r)} r_0{}^2 dx + \int_{F(r)}^x r^2 dx}{r^2 x}} = \sqrt{\frac{G + x}{x}}$$

One can show by use of the mean value theorem for integrals that:

$$\frac{1}{r^2} \int_0^{F(r)} r_0{}^2 dx \leq F(r)$$

Thus:

$$G = \text{constant} \leq 0$$

Hence, the heat-transfer parameter on the cylindrical afterbody approaches the flat-plate (constant-pressure) value asymptotically from above. Due to the presence of the nose, the afterbody is subjected to a "carry-over" of the heat-transfer parameter which amounts to a value greater than that which would have existed had the cylinder, for instance, been hollow (open-nosed).

Relation Between Two-Dimensional Compressible Flow and Two-Dimensional Incompressible Flow

In reference 25, Stewartson shows that the two-dimensional compressible boundary-layer equations for laminar flow (eqs. (B1) with $r_0 = r = $ constant) can be transformed into the two-dimensional incompressible boundary-layer equations provided that (1) the viscosity varies as the absolute temperature, (2) no heat is transferred, and (3) the Prandtl number is unity. In Stewartson's transformation the new variables are defined as follows:

(a) Independent-variable transformations

$$Y = \frac{a_1}{a_0 \sqrt{\nu_0}} \int_0^y \frac{\rho}{\rho_0}\, dy \qquad\qquad (B4a)$$

$$z = \int_{x_0}^{x} \left(\frac{a_1}{a_0} \right)^{\frac{3\gamma-1}{\gamma-1}} dx \qquad (B4b)$$

(b) Dependent-variable transformations:

$$\rho u = \rho_0 \sqrt{\nu_0} \, \frac{\partial \psi}{\partial y} \qquad (B5a)$$

$$\rho v = -\rho_0 \sqrt{\nu_0} \, \frac{\partial \psi}{\partial x} \qquad (B5b)$$

$$S = \frac{T - T_1 \left[1 + \frac{\gamma - 1}{2} \left(\frac{u_1^2 - u^2}{a_1^2} \right) \right]}{T_0 \left(1 + \frac{\gamma - 1}{2} M_0^2 \right)} \qquad (B5c)$$

$$V_1 = \frac{a_0 u_1}{a_1} = a_0 M_1 \qquad (B5d)$$

$$\mu = \frac{\mu_0 T}{T_0} \qquad (B5e)$$

$$\frac{\gamma - 1}{2} c_p \frac{dT_1}{dx} = a_1 \frac{da_1}{dx} = -\frac{\gamma - 1}{2} u_1 \frac{du_1}{dx} = \frac{\gamma - 1}{2} \frac{1}{\rho_1} \frac{dp_1}{dx} \qquad (B5f)$$

The subscript o refers to a standard state in the isentropic local free stream adjacent to the body. For convenience, this reference is later taken at the point where $x = 0$.

If only the first of Stewartson's three assumptions is retained and the remaining two are relaxed so that the Prandtl number is arbitrary but constant and if the body is no longer thermally insulated, the Stewartson transformations yield the following set of equations:

$$\frac{\partial^3 \psi}{\partial Y^3} - \frac{\partial \psi}{\partial Y} \frac{\partial^2 \psi}{\partial Y \partial z} + \frac{\partial \psi}{\partial z} \frac{\partial^2 \psi}{\partial Y^2} = -\frac{V_1 dV_1}{dz} (1 + S) \qquad (B6a)$$

$$\frac{\partial \psi}{\partial Y}\frac{\partial S}{\partial z} - \frac{\partial \psi}{\partial z}\frac{\partial S}{\partial Y} - \frac{1}{Pr}\frac{\partial^2 S}{\partial Y^2} = \left(\frac{Pr - 1}{Pr}\right)\left(\frac{\gamma - 1}{a_0{}^2 + \frac{\gamma - 1}{2}V_1{}^2}\right)\left\{\frac{\partial^2}{\partial Y^2}\left[\frac{1}{2}\left(\frac{\partial \psi}{\partial Y}\right)^2\right]\right\}$$

$$(B6b)$$

Equations (B6) differ in form from the corresponding set appropriate to two-dimensional incompressible flow. In contrast to their incompressible counterparts, equations (B6) must be solved, in general, as a simultaneous system because the momentum equation, equation (B6a), is not free of the temperature variable, S. However, equation (B6a) may be approximated by its incompressible analogue if the stipulation is introduced that the absolute value of the difference between the stagnation temperature and the surface temperature shall be small when compared to the stagnation temperature. Under this restriction the temperature variable, S, can be shown to be small when compared to unity throughout the boundary layer and the momentum equation is, for practical purposes, independent of the energy equation, just as in incompressible flow. It is easily seen that the foregoing assumption leads to the requirement of an isothermal surface.

A minor difference between the energy equation, equation (B6b), and the corresponding incompressible form may be found in the second factor on the right-hand side of equation (B6b). This difference can be eliminated by restricting the Prandtl number to a value of unity, in which case the right-hand sides of both the compressible and the incompressible equation become identically zero. The assumption of unity for Prandtl number is, however, deemed unnecessary to a solution of the heat-transfer problem because, as has been discussed in reference 6 with regard to a similar form of the energy equation, equation (B6b) is linear in S, and its complete solution may be found in such a way that its particular integral satisfies only the boundary conditions for the insulated surface condition. Thus, the nonzero heat-transfer case for arbitrary Prandtl numbers can be assumed to be given by the complementary solution to equation (B6b), and the necessity for solving the extremely complicated equations (B6) as they stand can be avoided for heat transfer at an isothermal surface.

Since equations (B6) are equivalent to their incompressible counterparts when restricted as indicated above, the transformation of Stewartson, equations (B4) and (B5), can be used to evaluate the second factor on the right-hand side of equation (2) of the text, if nomenclature is changed as follows:

$$\sqrt{\nu_0}\ Y = \bar{\bar{y}} \qquad\qquad (B7a)$$

$$z = \bar{x} \qquad\qquad (B7b)$$

$$V_1 = \bar{\bar{u}}_1 \qquad\qquad (B7c)$$

From equation (1) of the text, and definitions given in Appendix A, the heat-transfer parameter for incompressible, constant-property flow is found to be:

$$\frac{\overline{\overline{Nu}}}{\sqrt{\overline{\overline{Re}}}} = \frac{\overline{\overline{q}}\,\overline{\overline{x}}}{\overline{\overline{k}}_0\left(\overline{\overline{T}}_s - \overline{\overline{T}}_e\right)}\left(\frac{\overline{\overline{v}}_0}{\overline{\overline{xu}}_1}\right)^{1/2} = -\frac{\left(\dfrac{\partial\overline{\overline{T}}}{\partial\overline{\overline{y}}}\right)_s}{\left(\overline{\overline{T}}_s - \overline{\overline{T}}_e\right)}\left(\frac{\overline{\overline{v}}_0\,\overline{\overline{x}}}{\overline{\overline{u}}_1}\right)^{1/2}$$

And the heat-transfer parameter for two-dimensional compressible flow is:

$$\frac{\overline{Nu}}{\sqrt{\overline{\overline{Re}}}} = \frac{\left(\dfrac{\overline{h}\overline{x}}{\widetilde{k}_1}\right)}{\left(\dfrac{\overline{u}_1\overline{x}}{\overline{v}_1}\right)^{1/2}} = -\frac{\widetilde{k}_s}{\widetilde{k}_1}\frac{\left(\dfrac{\partial\overline{T}}{\partial\overline{y}}\right)_s}{\left(\overline{T}_s - \overline{T}_e\right)}\left(\frac{\overline{v}_1\overline{x}}{\overline{u}_1}\right)^{1/2}$$

The ratio between two-dimensional compressible and two-dimensional incompressible heat-transfer parameters becomes:

$$\frac{\overline{Nu}/\sqrt{\overline{Re}}}{\overline{\overline{Nu}}/\sqrt{\overline{\overline{Re}}}} = \frac{\left(\dfrac{\partial\overline{T}}{\partial\overline{y}}\right)_s}{\left(\dfrac{\partial\overline{\overline{T}}}{\partial\overline{\overline{y}}}\right)_s}\frac{\widetilde{k}_s}{\widetilde{k}_1}\left(\frac{\overline{\overline{T}}_s - \overline{\overline{T}}_e}{\overline{T}_s - \overline{T}_e}\right)\left(\frac{\overline{v}_1\,\overline{\overline{x}}\overline{\overline{u}}_1}{\overline{\overline{v}}_0\,\overline{\overline{x}}\overline{u}_1}\right)^{1/2}$$

But, as a result of equations (B4) and (B5) and the assumed temperature-viscosity law the following equalities hold:

$$\frac{\overline{a}_1}{\overline{a}_0} = \left(\frac{\overline{p}_1}{p_0}\right)^{\frac{\gamma-1}{2\gamma}}$$

$$\frac{\overline{\rho}_s}{\overline{\rho}_0} = \frac{\overline{p}_1}{\overline{p}_0}\frac{\overline{T}_0}{\overline{T}_s}$$

$$\frac{\overline{v}_1}{\overline{v}_0} = \frac{\overline{T}_1{}^2}{\overline{T}_0{}^2}\frac{\overline{p}_0}{\overline{p}_1}$$

$$\frac{\overline{k}_s}{\overline{k}_1} = \frac{\overline{T}_s}{\overline{T}_1}$$

$$\frac{\partial}{\partial \overline{y}} = \frac{\overline{a}_1}{\overline{a}_0} \cdot \frac{1}{\sqrt{\overline{v}_0}}\frac{\overline{\rho}}{\overline{\rho}_0}\frac{\partial}{\partial Y}$$

$$\frac{\partial}{\partial \overline{\overline{y}}} = \frac{1}{\sqrt{\overline{\overline{v}}_0}}\frac{\partial}{\partial Y}$$

It follows that

$$\frac{\overline{Nu/\sqrt{Re}}}{\overline{\overline{Nu/\sqrt{Re}}}} = \frac{\dfrac{\overline{a}_1}{\overline{a}_0}\dfrac{1}{\sqrt{\overline{v}_0}}\dfrac{\overline{\rho}_s}{\overline{\rho}_0}\left(\dfrac{\partial \overline{T}}{\partial Y}\right)_s}{\dfrac{1}{\sqrt{\overline{\overline{v}}_0}}\left(\dfrac{\partial \overline{\overline{T}}}{\partial Y}\right)_s}\frac{\overline{T}_s}{\overline{T}_1}\left(\frac{\overline{\overline{T}}_s - \overline{\overline{T}}_e}{\overline{T}_s - \overline{T}_e}\right)\left(\frac{\overline{v}_0\overline{T}_1{}^2}{\overline{\overline{T}}_0{}^2\overline{\overline{v}}_0}\frac{\overline{p}_0}{\overline{p}_1}\frac{\overline{\overline{u}}_1}{\frac{\overline{a}_1}{\overline{a}_0}\overline{\overline{u}}_1}\frac{\overline{x}}{\overline{\overline{x}}}\right)^{1/2}$$

For the same temperatures in both flows this expression can be readily simplified to

$$\frac{\overline{Nu/\sqrt{Re}}}{\overline{\overline{Nu/\sqrt{Re}}}} = \left(\frac{\overline{p}_1}{\overline{p}_0}\frac{\overline{a}_1}{\overline{a}_0}\frac{\overline{x}}{\overline{\overline{x}}}\right)^{1/2}$$

And, with further reduction, equation (4) of the text results. Equation (4) can be evaluated in terms of the streamwise coordinate, x, in the axisymmetric plane with the aid of Mangler's transformation. However, due to the complicated expression which may result in the general case, it has been found convenient to approximate equation (4) with another equation which is much more amenable to calculation. The manner in which this is accomplished will be discussed later.

Heat-Transfer Parameter in Two-Dimensional
Incompressible Flow

For convenience, heat-transfer solutions to the incompressible wedge-flow problem are selected to provide numerical values for the last factor on the right-hand side of equation (2) of the text. The differential equations which give rise to these solutions can be obtained from equations (B6) restricted to the previously discussed conditions under which Stewartson's transformation is valid. With the aid of the following substitutions

$$V_1 = \beta z^m \tag{B8a}$$

$$\psi = \left(\frac{2zV_1}{m+1}\right)^{1/2} \cdot f(\eta) \tag{B8b}$$

$$\eta = Y\left[\frac{(m+1)V_1}{2z}\right]^{1/2} \tag{B8c}$$

$$S = s \cdot S_s = sBz^\lambda \tag{B8d}$$

equations (B6) can be manipulated into the following forms:

$$f''' + ff'' = \frac{2m}{m+1}\left[(f')^2 - (1+S)\right] \tag{B9a}$$

$$s'' + Prfs' - \frac{2Pr\lambda f's}{m+1} = \left(\frac{1-Pr}{S_s}\right)\left[\frac{(\gamma-1)V_1^2}{a_0^2 + \frac{\gamma-1}{2}V_1^2}\right]\frac{d^2}{d\eta^2}\left[\frac{(f')^2}{2}\right] \tag{B9b}$$

where primes denote differentiation with respect to η. When the temperature variable, S, is assumed small compared to unity throughout the boundary layer, and the surface temperature is accordingly taken to be uniform $(\lambda = 0)$, and, furthermore, when one seeks only complementary solutions to the energy equation, equations (B9) may be approximated by:

$$f''' + ff'' = \frac{2m}{m+1}\left[(f')^2 - 1\right] \qquad \text{(B10a)}$$

$$s'' + Prfs' = 0 \qquad \text{(B10b)}$$

The applicable boundary conditions are:

$$\eta = 0: \quad f = f' = 0; \quad s = 1 \qquad \text{(B11a)}$$

$$\eta \longrightarrow \infty: \quad f' \longrightarrow 1; \quad s \longrightarrow 0 \qquad \text{(B11b)}$$

Equations (B10) and the associated boundary conditions (eqs. (B11))
constitute a formulation of the isothermal, incompressible, wedge-flow
problem. Heat-transfer solutions are known for a range of values of
Prandtl number and pressure-gradient parameter and are tabulated in ref-
erences 10 and 11. The incompressible heat-transfer parameter arising
from these solutions can be written:

$$\overline{\overline{Nu}}/\sqrt{\overline{\overline{Re}}} = -\,\overline{\overline{s}}'_s\,\sqrt{\frac{\overline{\overline{m}}+1}{2}} \qquad \text{(B12)}$$

The symbol $\overline{\overline{s}}'_s$ is the dimensionless temperature gradient across the
surface and is tabulated in reference 10 as θ'_w and in reference 11 as
$d\theta/d\eta\big|_{\eta=0}$. According to these calculations, the temperature gradient
across the surface, $\overline{\overline{s}}'_s$, is a function of the pressure-gradient parameter,
$\overline{\overline{m}}$, and the Prandtl number, Pr, but for a given wedge at a given Prandtl
number the pressure-gradient parameter and the heat-transfer parameter
are constant. Although these solutions are rigorously applicable to
wedges only, it has been shown (ref. 12, for example) that, on two-
dimensional bodies other than wedges, they adequately predict measured
distributions of the heat-transfer parameter which correspond to the
measured distributions of the pressure-gradient parameter. Thus, the
incompressible heat-transfer-parameter distribution for any body can be
estimated by means of equation (B12) and the tables of references 10 and
11 if the distribution of pressure-gradient parameter is known. To make
use of this in the present case, however, the incompressible pressure-
gradient parameter $\overline{\overline{m}}$ must be related to the axisymmetric compressible
pressure-gradient parameter m.

Relation Between Two-Dimensional Incompressible and Axisymmetric, Compressible Pressure-Gradient Parameters

The pressure-gradient transformation factors on the right-hand side of equation (6) of the text are evaluated by using the transformations of Stewartson and Mangler. In a manner similar to that already used to calculate the heat-transfer transformation factors, it is readily found that

$$\frac{\bar{\bar{m}}}{\bar{m}} = \left[\frac{\displaystyle\int_{\bar{x}_O}^{\bar{x}} \left(\frac{\bar{a}_1}{\bar{a}_O}\right)^{\frac{3\gamma-1}{\gamma-1}} d\bar{x}}{\bar{x}\left(\frac{\bar{a}_1}{\bar{a}_O}\right)^{\frac{3\gamma-1}{\gamma-1}}} \right] \left(1 + \frac{M_1{}^2}{5}\right) \tag{B13a}$$

$$\frac{\bar{m}}{m} = \frac{\displaystyle\int_{x_O}^{x} r_O{}^2 dx}{x\, r_O{}^2} \tag{B13b}$$

It should be noted that these pressure-gradient factors are functionally related to the heat-transfer-parameter factors given by equations (3) and (4) of the text. The factor represented by equation (B13b) can be evaluated for a body of revolution of given shape. The factor represented by equation (B13a) can be found in terms of the given axisymmetric streamwise coordinate x by virtue of Mangler's transformation, as was indicated for the case of equation 4. Because this procedure usually results in an expression of such complexity that numerical methods are required to effect the integrations, it is convenient to approximate equations (B13a) and (4) by simpler expressions which can be integrated once and for all.

Approximation of Pressure-Gradient-Parameter and Heat-Transfer-Parameter Transformation Factors Between Two-Dimensional Compressible and Incompressible Flows

Because heat-transfer solutions to the incompressible wedge-flow problem are utilized to provide numerical values for the last factor on the right-hand side of equation (2) of the text, it is consistent to treat the pressure-gradient parameters $\bar{\bar{m}}$ and $\bar{m}$ as constants during integration of equations (4) and (B13a), even though they are subsequently allowed to vary.

Setting γ equal to 1.4 and using the relations

$$\frac{\bar{a}_1}{\bar{a}_O} = \left(\frac{1 + \dfrac{M_O^2}{5}}{1 + \dfrac{M_1^2}{5}}\right)^{1/2}$$

$$d\bar{\bar{x}} = \left(\frac{1 + \dfrac{M_O^2}{5}}{1 + \dfrac{M_1^2}{5}}\right)^4 d\bar{x}$$

$$\bar{a}_1 = \sqrt{\bar{a}_O^2 + \frac{u_O^2}{5} - \frac{u_1^2}{5}}$$

$$M_1 = \frac{\bar{\beta}\,\bar{x}^{\bar{m}}}{\bar{a}_1} = \frac{\bar{\bar{\beta}}\,\bar{\bar{x}}^{\bar{\bar{m}}}}{\bar{a}_O}$$

to evaluate terms in equations (4) and (B13a) gives rise to the following two integrals:

$$\int_0^{\bar{x}} \left(\frac{\bar{a}_1}{\bar{a}_O}\right)^8 d\bar{x} = \int_0^{\bar{x}} \left[1 + \frac{M_O^2}{5} - \left(\frac{\bar{\beta}\,\bar{x}^{\bar{m}}}{\sqrt{5}\bar{a}_O}\right)^2\right]^4 d\bar{x} \qquad (B14a)$$

$$\int_0^{\bar{x}} d\bar{x} = \int_0^{\bar{\bar{x}}} \left[1 + \left(\frac{\bar{\bar{\beta}}\,\bar{\bar{x}}^{\bar{\bar{m}}}}{\sqrt{5}\bar{a}_O}\right)^2\right]^4 d\bar{\bar{x}} \qquad (B14b)$$

For convenience, the lower limit of these integrals has been set equal to zero. After evaluation of the integrals (eqs. (B14)), by assuming

that the pressure-gradient parameters are not functions of the coordinates, approximate values for the factors on the right-hand sides of equations (B13a) and (4) are found.

$$\frac{\overline{Nu}/\sqrt{\overline{Re}}}{\overline{\overline{Nu}}/\sqrt{\overline{\overline{Re}}}} = \sqrt{\frac{1 + \frac{4}{2\overline{\overline{m}}+1}\left(\frac{M_1^2}{5}\right) + \frac{6}{4\overline{\overline{m}}+1}\left(\frac{M_1^2}{5}\right)^2 + \frac{4}{6\overline{\overline{m}}+1}\left(\frac{M_1^2}{5}\right)^3 + \frac{1}{8\overline{\overline{m}}+1}\left(\frac{M_1^2}{5}\right)^4}{\left(1 + \frac{M_1^2}{5}\right)^4}}$$

(B15a)

and

$$\frac{\overline{\overline{m}}}{\overline{m}} = \left(1 + \frac{M_1^2}{5}\right)\left[\frac{1 - \frac{4}{2\overline{m}+1}\left(\frac{M_1^2}{5+M_1^2}\right) + \frac{6}{4\overline{m}+1}\left(\frac{M_1^2}{5+M_1^2}\right)^2 - \frac{4}{6\overline{m}+1}\left(\frac{M_1^2}{5+M_1^2}\right)^3 + \frac{1}{8\overline{m}+1}\left(\frac{M_1^2}{5+M_1^2}\right)^4}{\left(1 - \frac{M_1^2}{5+M_1^2}\right)^4}\right]$$

(B15b)

provided that $\overline{\overline{m}} > -\frac{1}{8}$; $\overline{m} > -\frac{1}{8}$

From equations (B15) it can be observed that the local heat-transfer parameter in two-dimensional compressible flow with favorable pressure gradient $(\overline{m}, \overline{\overline{m}} > 0)$ decreases with Mach number and, except at the forward stagnation point, is less than the corresponding local heat-transfer parameter in incompressible flow. There is no change predicted with Mach number on constant-pressure surfaces $(\overline{m}, \overline{\overline{m}} = 0)$. Conversely, the pressure-gradient parameter $\overline{\overline{m}}$ in the two-dimensional incompressible flow, corresponding to a favorable pressure-gradient parameter $\overline{m}$ in the two-dimensional compressible flow, increases with Mach number.

It should be noted that equations (B15a) and (B15b) are equivalent, and can be related through equations (4) and (B13a) as follows:

$$\frac{\bar{\bar{m}}}{\bar{m}} = \left(1 + \frac{M_1{}^2}{5}\right)\left(\frac{\overline{\overline{Nu/\sqrt{Re}}}}{\overline{Nu/\sqrt{Re}}}\right)^2 \qquad (B16)$$

Application of the Method

In utilizing the foregoing method for calculating any local value of the laminar heat-transfer parameter on a body of revolution with iso-thermal surface in a compressible flow, a procedure may be followed as outlined below:

1. For a given point on a body of revolution about which the local isentropic flow is known, the pressure-gradient parameter m is computed from equation (7); and the transformation factors $\dfrac{Nu/\sqrt{Re}}{\overline{Nu/\sqrt{Re}}}$ and $\dfrac{\bar{m}}{m}$ are computed from equations (3) and/or (B13b).

2. After evaluating the pressure-gradient parameter $\bar{m}$ corresponding to the two-dimensional compressible flow by combining equations (7) and (B13b), the transformation factor $\dfrac{\bar{\bar{m}}}{\bar{m}}$ can be calculated for the desired point from equation (B15b).

3. A value of the incompressible pressure-gradient parameter $\bar{\bar{m}}$ is obtained by combining equations (7), (B13b), and (B15b) as indicated in equation (6), after which it is possible to evaluate equation (B12) for a given Prandtl number with the aid of the tables of references 10 and 11.

4. Using the pressure-gradient parameter $\bar{\bar{m}}$ equation (B15a) is evaluated at the desired point for the known Mach number, M_1. An alternate, and quicker, method is to utilize equation (B16) in conjunction with the results of item (2) above.

5. A combination of the results of items (1), (3), and (4) above according to equation (2) yields the desired local value of the axisymmetric compressible heat-transfer parameter.

Point-by-point repetition of this procedure provides a distribution of isothermal heat-transfer parameter over the surface of the body of revolution. Such a distribution is shown in figure 4(b) for the case of a hemisphere-cylinder at a free-stream Mach number of 1.97.

REFERENCES

1. Kaye, Joseph: The Transient Temperature Distribution in a Wing Flying at Supersonic Speeds. Jour. Aero. Sci., vol. 17, no. 12, Dec. 1950, pp. 787-807.

2. Mangler, W.: Compressible Boundary Layers on Bodies of Revolution. M.A.P. Völkenrode Rep. VG 83, No. 47T., Mar. 15, 1946.

3. Moore, L. L.: A Solution of the Laminar Boundary-Layer Equations For a Compressible Fluid With Variable Properties, Including Dissociation. Jour. Aero. Sci., vol. 19, no. 8, Aug. 1952, pp. 505-518.

4. Young, George B. W., and Janssen, Earl: The Compressible Boundary Layer. Jour. Aero. Sci., vol. 19, no. 4, Apr. 1952, pp. 229-236.

5. Klunker, E. B., and McLean, F. Edward: Effect of Thermal Properties on Laminar-Boundary-Layer Characteristics. NACA TN 2916, 1953.

6. Chapman, Dean R., and Rubesin, Morris W.: Temperature and Velocity Profiles in the Compressible Laminar Boundary Layer With Arbitrary Distribution of Surface Temperature. Jour. Aero. Sci., vol. 16, no. 9, Sept. 1949, pp. 547-565.

7. Ferrari, Carlo: Velocity and Temperature Distribution Through the Laminar Boundary Layer in Supersonic Flow. Jour. Aero. Sci., vol. 19, no. 1, Jan. 1952, pp. 39-47.

8. Tani, Itiro: Further Studies of the Laminar Boundary Layer in Compressible Fluids. Rep. No. 322 (vol. 22, no. 23), Aero. Res. Inst., Tokyo Imperial Univ., Dec. 1944.

9. Low, George M.: The Compressible Laminar Boundary Layer With Heat Transfer and Small Pressure Gradient. NACA TN 3028, 1953.

10. Brown, W. Byron, and Donoughe, Patrick L.: Tables of Exact Laminar-Boundary-Layer Solutions When the Wall is Porous and Fluid Properties Are Variable. NACA TN 2479, 1951.

11. Levy, Solomon: Heat Transfer to Constant-Property Laminar Boundary-Layer Flows With Power-Function Free-Stream Velocity and Wall-Temperature Variation. Jour. Aero. Sci., vol. 19, no. 5, May 1952, pp. 341-348.

12. Eckert, E. R. G., and Livingood, John N. B.: Method for Calculation of Heat Transfer in Laminar Region of Air Flow Around Cylinders of Arbitrary Cross Section (Including Large Temperature Differences and Transpiration Cooling). NACA TN 2733, 1952.

13. Bryson, A. E., and Edwards, R. H.: The Effect of Nonuniform Surface
    Temperature on the Transient Aerodynamic Heating of Thin-Skinned
    Bodies. Jour. Aero. Sci., vol. 19, no. 7, July 1952, pp. 471-475.

14. Scherrer, Richard, Wimbrow, William R., and Gowen, Forrest E.:
    Heat-Transfer and Boundary-Layer Transition on a Heated 20° Cone
    at a Mach Number of 1.53. NACA RM A8L28, 1949.

15. Scherrer, Richard, and Gowen, Forrest E.: Comparison of Theoretical
    and Experimental Heat Transfer on a Cooled 20° Cone With a Laminar
    Boundary Layer at a Mach Number of 2.02. NACA TN 2087, 1950.

16. Slack, Ellis G.: Experimental Investigation of Heat Transfer Through
    Laminar and Turbulent Boundary Layers on a Cooled Flat Plate at a
    Mach Number of 2.4. NACA TN 2686, 1952.

17. Eber, G. R.: Recent Investigation of Temperature Recovery and Heat
    Transmission on Cones and Cylinders in Axial Flow in the NOL Aero-
    ballistic Wind Tunnel. Jour. Aero. Sci., vol. 19, no. 1, Jan. 1952,
    pp. 1-6, 14.

18. Scherrer, Richard: Comparison of Theoretical and Experimental Heat-
    Transfer Characteristics of Bodies of Revolutions at Supersonic
    Speeds. NACA Rep. 1055, 1951.

19. Wimbrow, William R., and Scherrer, Richard: Laminar-Boundary-Layer
    Heat-Transfer Characteristics of a Body of Revolution with a
    Pressure Gradient at Supersonic Speeds. NACA TN 2148, 1950.

20. Korobkin, Irving: Local Flow Conditions, Recovery Factors and Heat-
    Transfer Coefficients on the Nose of a Hemisphere-Cylinder at a
    Mach Number of 2.8. NAVORD Rep. 2865 (Aeroballistics Res. Rep.
    175), Whiteoak, Md., May 5, 1953.

21. Levy, Solomon, and Seban, R. A.: Recovery Factors for the Laminar
    "Separation" and Stagnation Flows. Jour. Aero. Sci., vol. 19,
    no. 5, May 1952, pp. 55-57.

22. Sibulkin, Merwin: Heat Transfer Near the Forward Stagnation Point
    of a Body of Revolution. Jour. Aero. Sci., vol. 19, no. 8,
    Aug. 1952, pp. 570-571.

23. Morduchow, Morris: On Heat Transfer Over a Sweat-Cooled Surface in
    Laminar Compressible Flow With a Pressure Gradient. Jour. Aero.
    Sci., vol. 19, no. 10, Oct. 1952, pp. 705-712.

24. Drake, Robert M., Jr.: Calculation Method for Three-Dimensional
    Rotationally Symmetrical Laminar Boundary Layers With Arbitrary
    Free-Stream Velocity and Arbitrary Wall-Temperature Variation.
    Jour. Aero. Sci., vol. 20, no. 5, 1953, pp. 309-316, 330.

25. Stewartson, K.: Correlated Incompressible and Compressible Boundary
    Layers. Proc. Royal Soc. (of London) Ser. A, v. 200, 1949,
    pp. 84-100.

26. Morey, F. C.: The NBS-NACA Tables of Thermal Properties of Gases,
    Tables 2.39, Dry Air Coefficients of Viscosity; Nuttall, R. L.:
    The NBS-NACA Tables of Thermal Properties of Gases, Tables 2.42,
    Dry Air Thermal Conductivity. National Bureau of Standards, 1950.

27. Grimminger, G., Williams, E. P., and Young, G. B. W.: Lift on
    Inclined Bodies of Revolution in Hypersonic Flow. Jour. Aero
    Sci., vol. 17, no. 11, Nov. 1950, pp. 675-690.

28. Oswatitsch, Klaus: Similarity Laws for Hypersonic Flow. Kungl.
    Tekniska Högskolan, Stockholm. Institutionen för Flygteknik
    Tech. Note 16, July 19, 1950. See also: Zeitschrift für
   angewandte Mathematik und Physik, v. 2, 1951, p. 249-264.

TABLE I.- TEST CONDITIONS

| Test	Wind tunnel	Mach number M_∞	Reynolds number Re_D, million	Stagnation temperature $T_t(^\circ R)$
Pressure distribution	1 2	1.97 1.97 3.04 3.80	0.58 to 2.23 2.91 to 6.61 2.79 to 4.05 2.84	544-572 variable variable variable
Temperature distribution	1 2	1.97 1.97 3.04	0.58 to 2.3 3.12 to 4.16 2.85 to 3.31	527-571 variable variable
Heat-transfer distribution	1	1.97	0.60 1.19 1.73 2.28	530 544 557 570
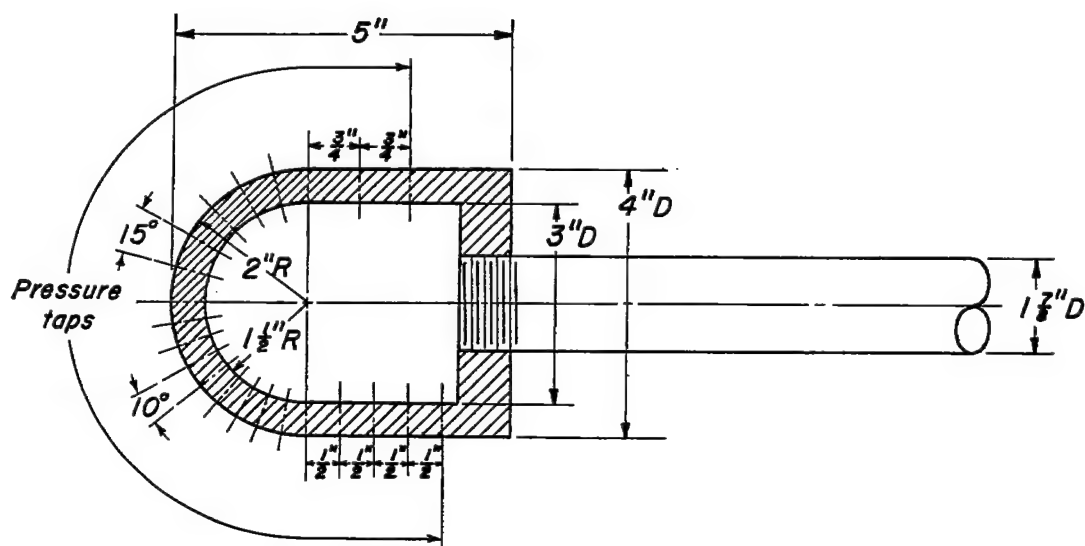
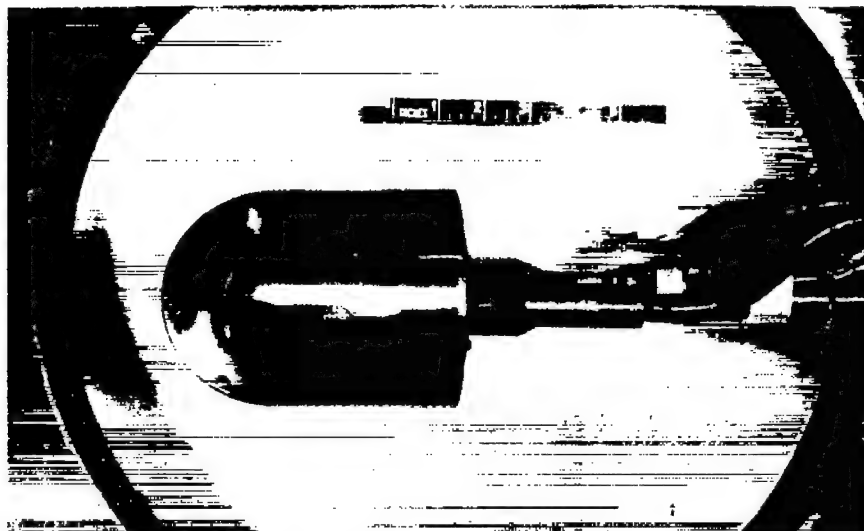(a) Pressure-distribution model.
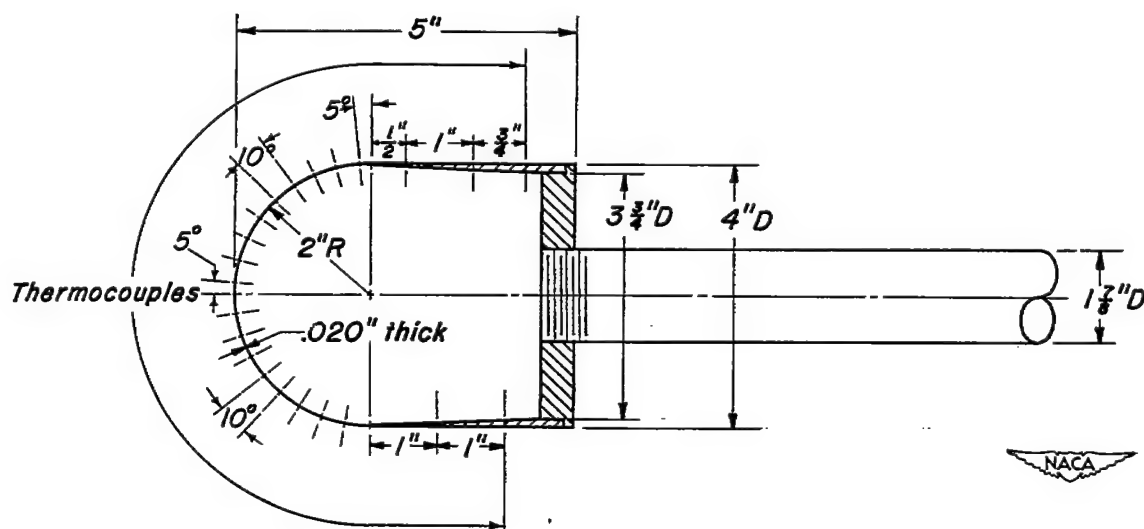
(b) Recovery-factor model.

Figure 1.- Hemisphere-cylinder.
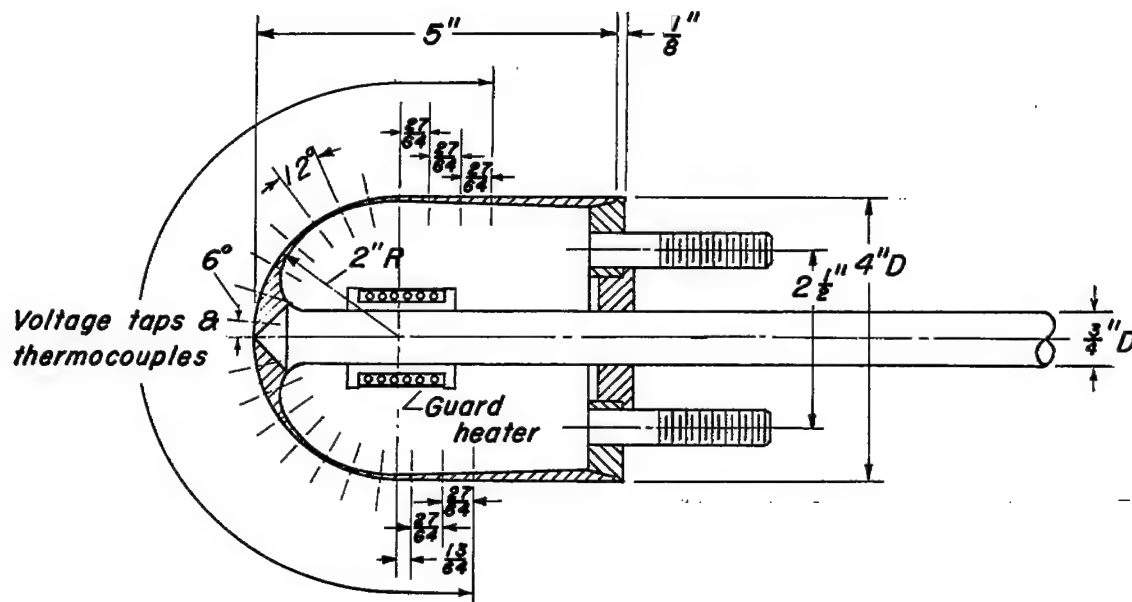
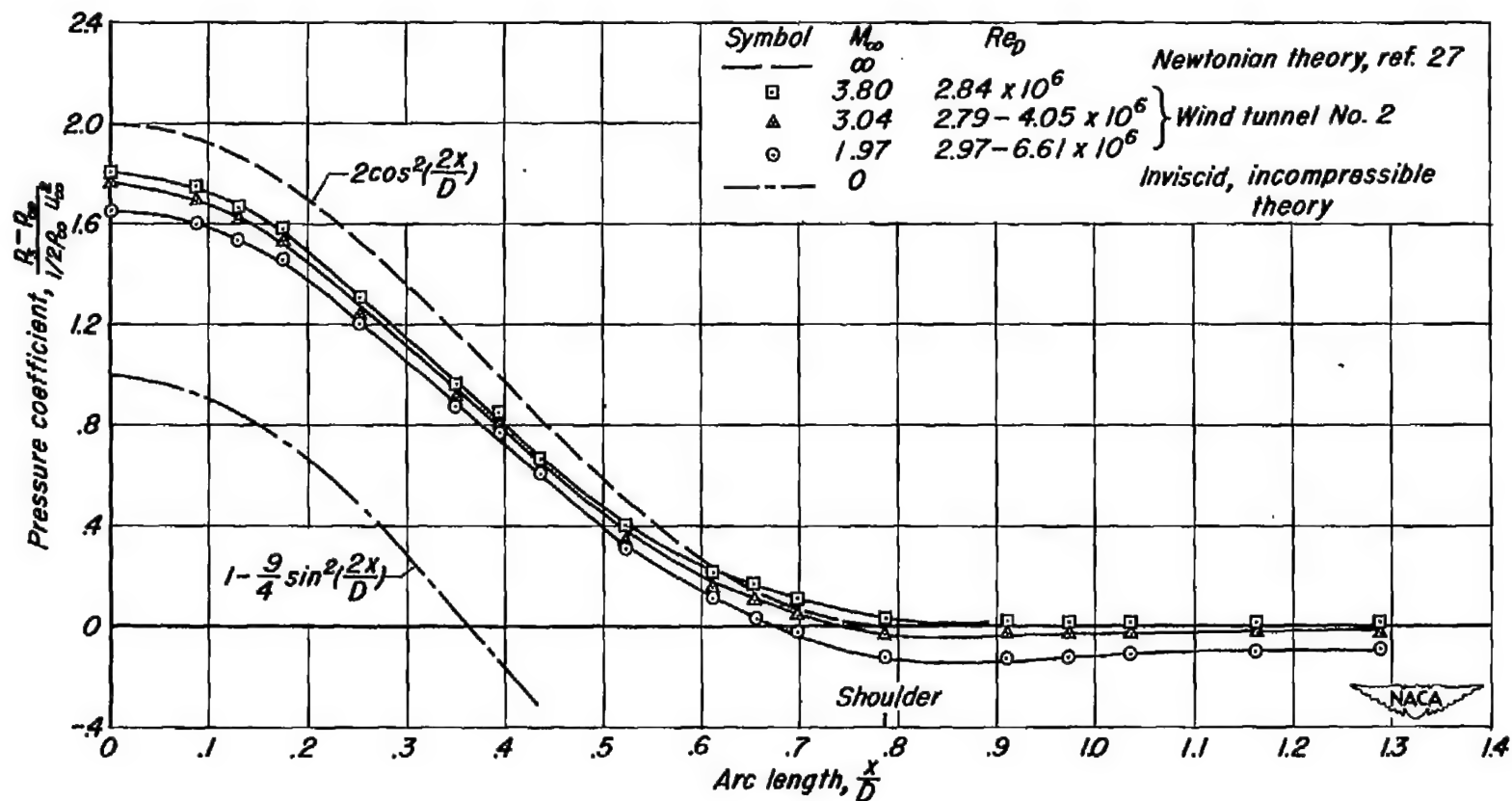(c) Heat-transfer model (electrically heated).

A-18536

(d) Photograph of heat-transfer-model installation in the Ames
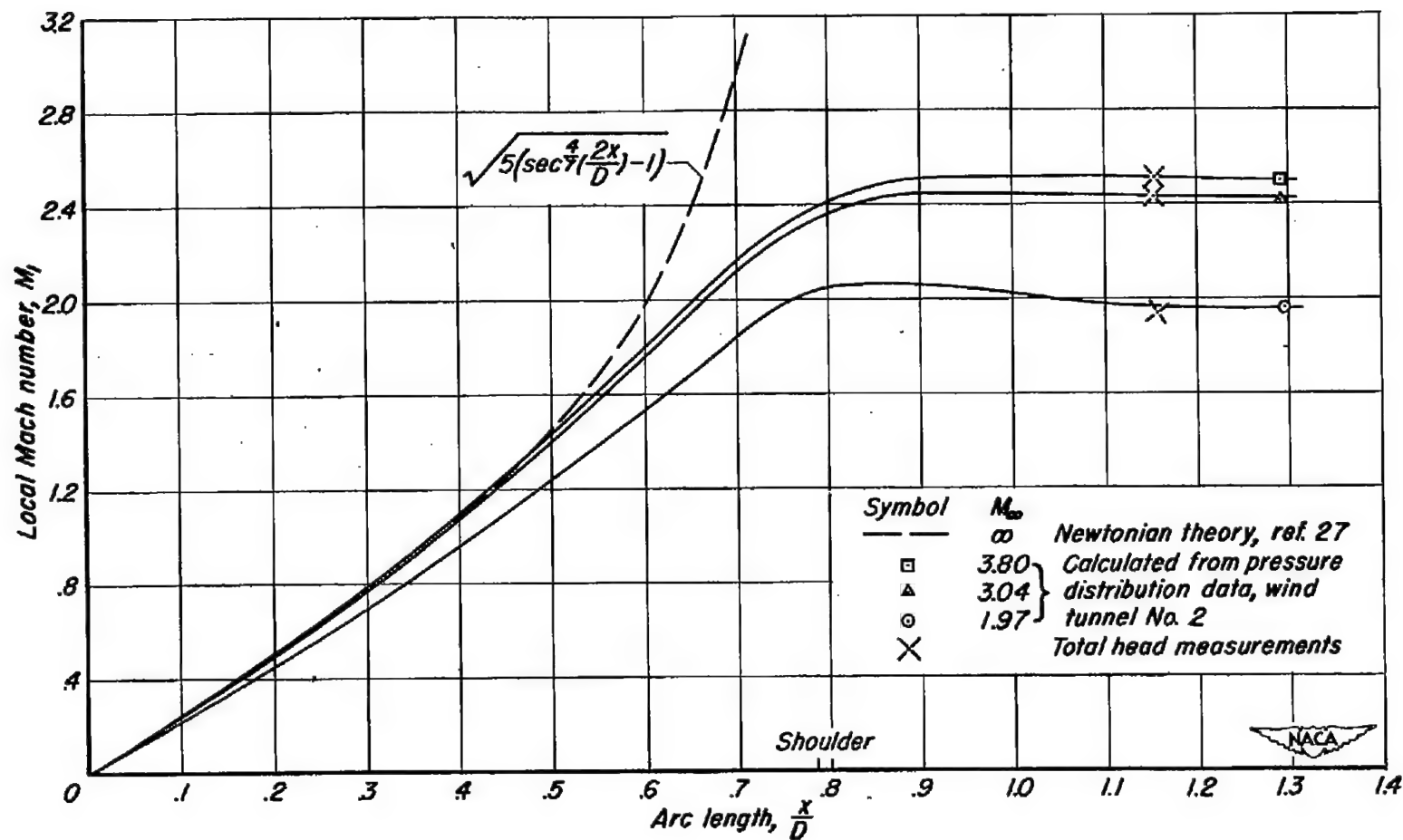1- by 3-foot supersonic wind tunnel No. 1.

Figure 1.- Concluded.
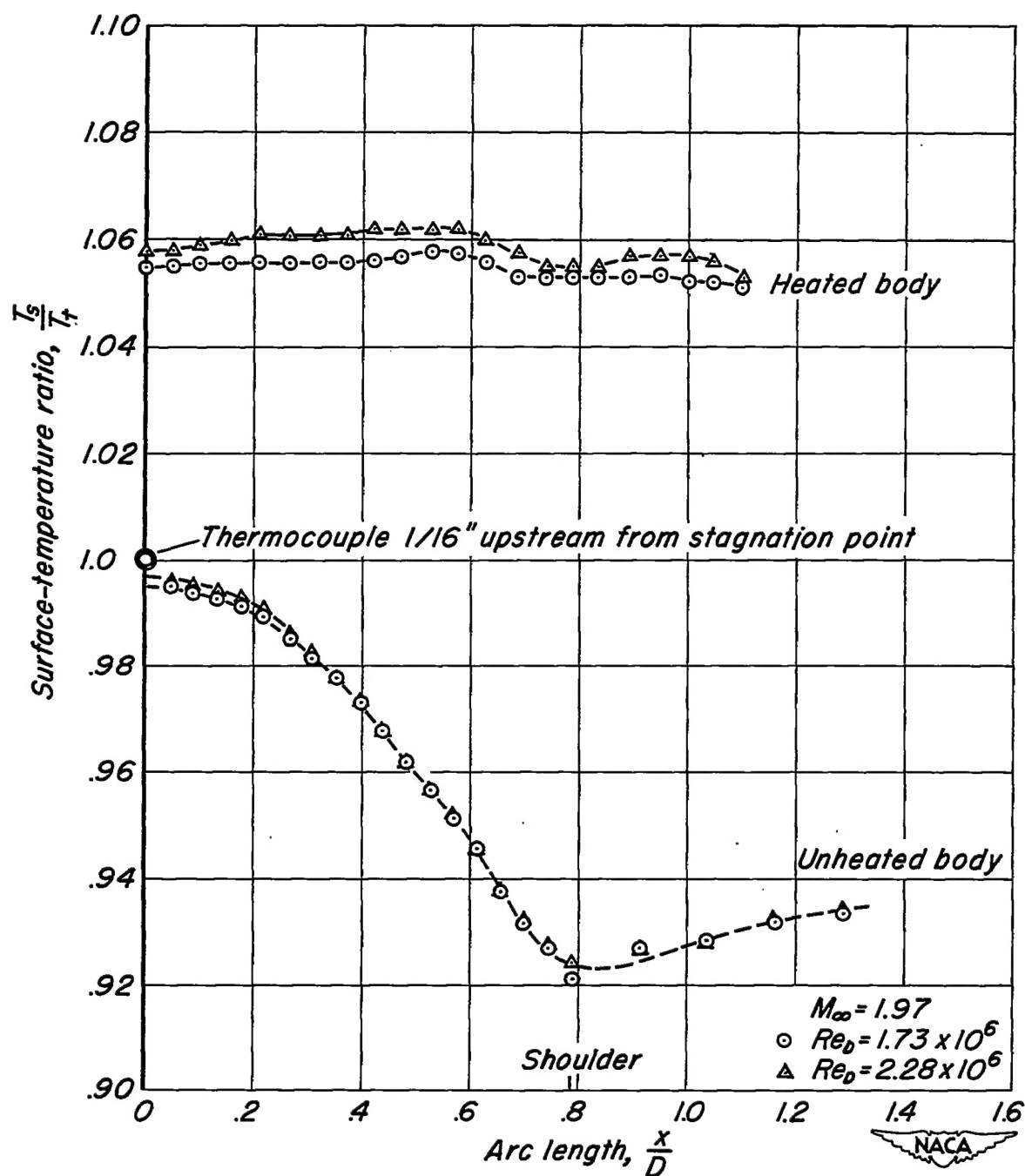
(a) Variation of pressure coefficient along surface.

Figure 2.- Results of pressure measurements on hemisphere-cylinder.

$$\sqrt{5\left(\sec^{\frac{4}{7}}\left(\frac{2x}{D}\right)-1\right)}$$

Symbol	M_∞	
— — —	∞	Newtonian theory, ref. 27
▫	3.80 ⎤	Calculated from pressure
▲	3.04 ⎬	distribution data, wind
⊙	1.97 ⎦	tunnel No. 2
✕		Total head measurements

Shoulder
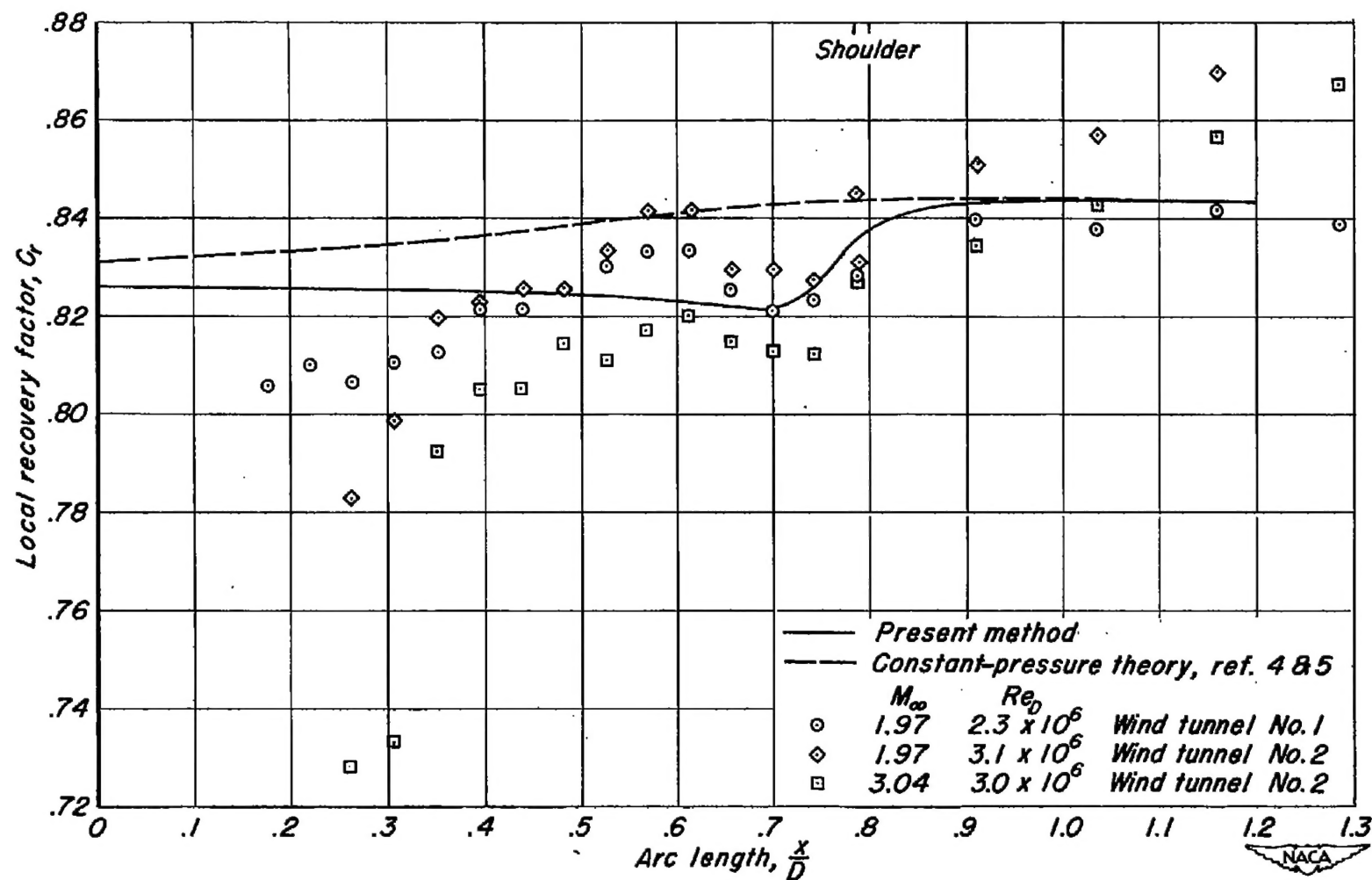
Local Mach number, M_l

Arc length, $\frac{x}{D}$

(b) Variation of local Mach number along surface.
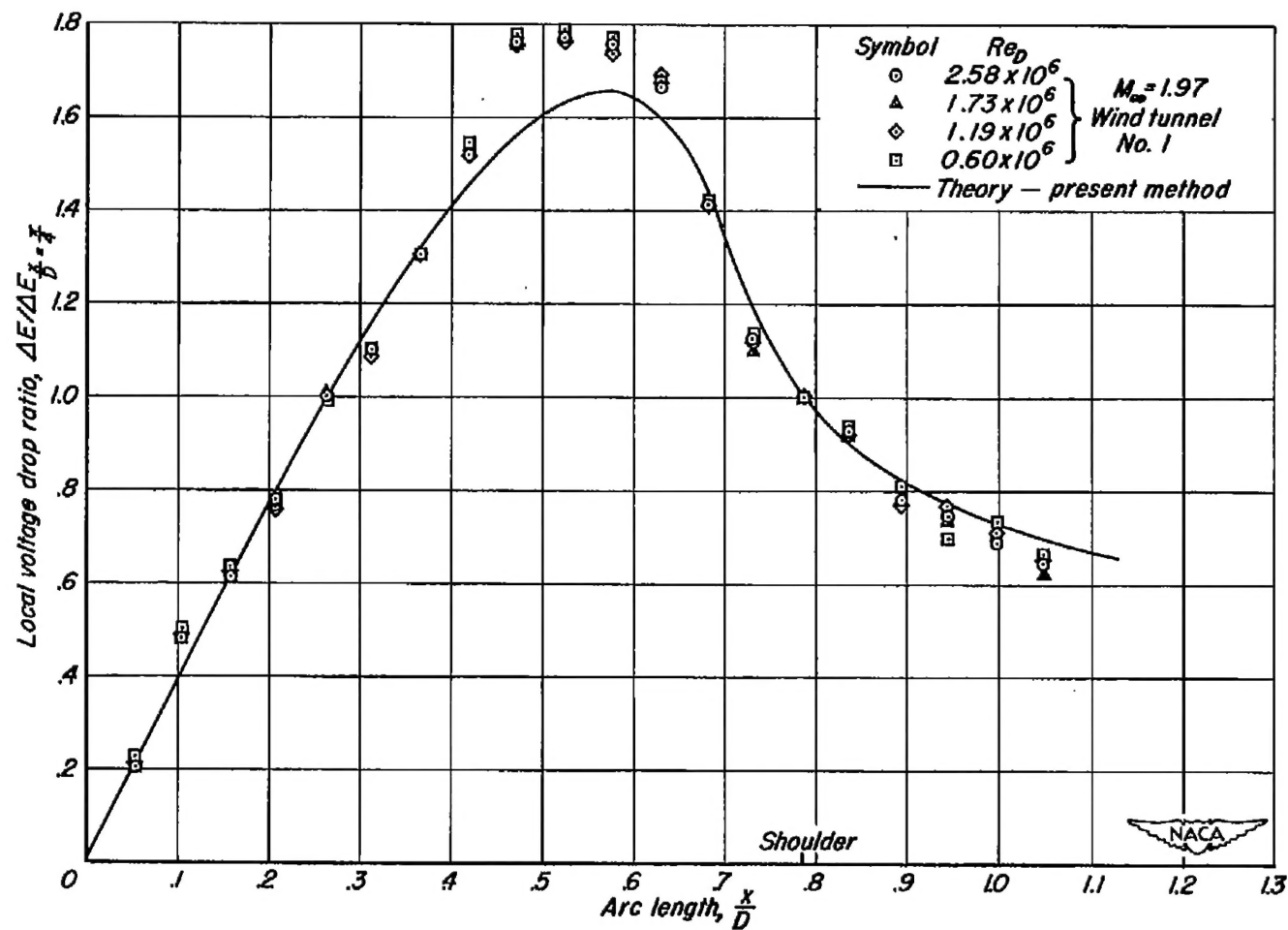
Figure 2.- Concluded.

(a) Variation of surface- to total-temperature ratio
along surface.

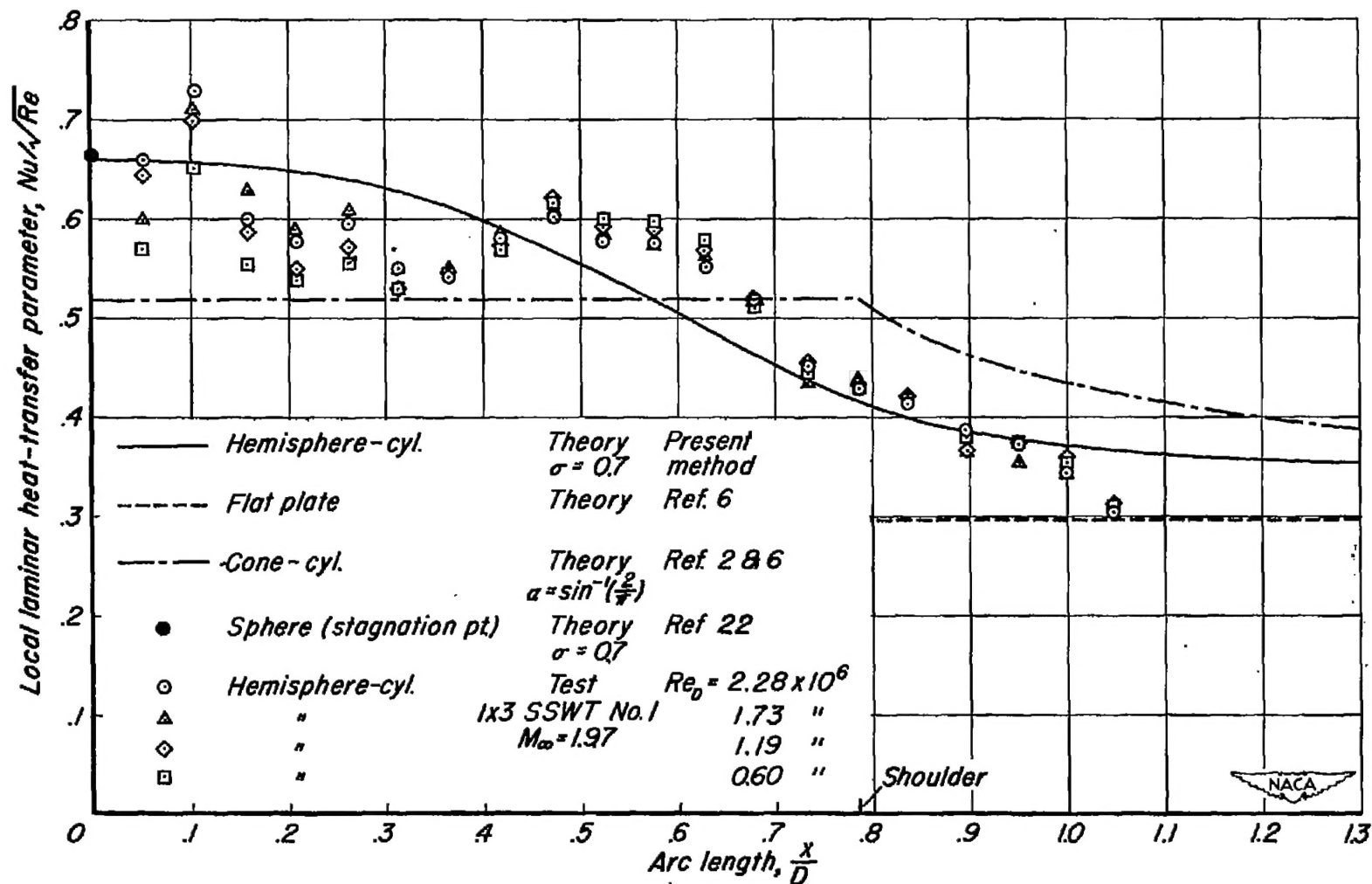Figure 3.- Results of temperature measurements on hemisphere-cylinder.

(b) Variation of local recovery factor along surface.

Figure 3.- Concluded.

(a) Variation of local voltage-drop ratio
along surface.

Figure 4.- Results of heat-transfer measurements on hemisphere-cylinder.

Local laminar heat-transfer parameter, $Nu/\sqrt{Re}$

.8

.7

.6

.5

.4

.3

.2

.1

——	Hemisphere – cyl.	Theory $\sigma = 0.7$	Present method
———	Flat plate	Theory	Ref. 6
—·—·	Cone – cyl.	Theory $a = \sin^{-1}\left(\frac{2}{\pi}\right)$	Ref. 2 & 6
●	Sphere (stagnation pt)	Theory $\sigma = 0.7$	Ref. 22
⊙	Hemisphere-cyl.	Test	$Re_D = 2.28 \times 10^6$
△	"	1x3 SSWT No.1	1.73 "
◇	"	$M_\infty = 1.97$	1.19 "
⊡	"		0.60 "

Shoulder

Arc length, $\frac{x}{D}$

0   .1   .2   .3   .4   .5   .6   .7   .8   .9   1.0   1.1   1.2   1.3

(b) Variation of local heat-transfer parameter along isothermal surface.

Figure 4.- Concluded.